www.elsevier.com/locate/developmentalbiology

Characterization of somatic embryogenesis initiated from the *Arabidopsis* shoot apex

Satoshi Kadokura, Kaoru Sugimoto, Paul Tarr, Takamasa Suzuki, Sachihiro Matsunaga

PII: S0012-1606(17)30802-3
DOI: https://doi.org/10.1016/j.ydbio.2018.04.023
Reference: YDBIO7751

To appear in: *Developmental Biology*

Received date: 30 November 2017
Revised date: 16 April 2018
Accepted date: 24 April 2018

Cite this article as: Satoshi Kadokura, Kaoru Sugimoto, Paul Tarr, Takamasa Suzuki and Sachihiro Matsunaga, Characterization of somatic embryogenesis initiated from the *Arabidopsis* shoot apex, *Developmental Biology,* https://doi.org/10.1016/j.ydbio.2018.04.023

Characterization of somatic embryogenesis initiated from the *Arabidopsis* shoot apex

Satoshi Kadokura[a 1], Kaoru Sugimoto[a1*], Paul Tarr[b], Takamasa Suzuki[c], Sachihiro Matsunaga[a*]

[a]Department of Applied Biological Science, Faculty of Science and Technology, Tokyo University of Science, 2641 Yamazaki, Noda, Chiba 278-8510, Japan

[b]Division of Biology 156-29, California Institute of Technology, Pasadena, California 91125, USA

[c]College of Bioscience and Biotechnology, Chubu University, 1200 Matsumoto-cho, Kasugai, Aichi 487-8501, Japan.

kaoru_sugimoto@rs.tus.ac.jp

sachi@rs.tus.ac.jp

*Corresponding authors: Phone: +81-4-7124-1501 (ext. 3442)

[1] These authors contributed equally to this work

Abstract

Somatic embryogenesis is one of the best examples of the remarkable developmental plasticity of plants, in which committed somatic cells can dedifferentiate and acquire the ability to form an embryo and regenerate an entire plant. In *Arabidopsis thaliana*, the shoot apices of young seedlings have been reported as an alternative tissue source for somatic embryos (SEs) besides the widely studied zygotic embryos taken from siliques. Although SE induction from shoots demonstrates the plasticity of plants more clearly than the embryo-to-embryo induction system, the underlying developmental and molecular mechanisms involved are unknown. Here we characterized SE formation from shoot apex explants by establishing a system for time-lapse observation of explants during SE induction. We also established a method to distinguish SE-forming and non-SE-forming explants prior to anatomical SE formation, enabling us to identify distinct transcriptome profiles of these two explants at SE initiation. We show that embryonic fate commitment takes place at day 3 of SE induction and the SE arises directly, not through callus formation, from the base of leaf primordia just beside the shoot apical meristem (SAM), where auxin accumulates and shoot-root polarity is formed. The expression domain of a couple of key developmental genes for the SAM transiently expands at this stage. Our data demonstrate that SE-forming and

non-SE-forming explants share mostly the same transcripts except for a limited number of embryonic genes and root genes that might trigger the SE-initiation program. Thus, SE-forming explants possess a mixed identity (SAM, root and embryo) at the time of SE specification.

Keywords:

somatic embryogenesis, *Arabidopsis thaliana*, stress treatment, shoot apical meristem, leaf primordia, fate conversion

1. Introduction

It is well known that plant cells are more plastic than animal cells, but the mechanisms that explain why plants have such remarkable developmental plasticity are not clear. Somatic embryogenesis is one of the best examples of the high plasticity of plants. During this process, committed somatic cells can dedifferentiate and acquire the ability to form an embryo; that is, to regenerate an entire plant (Mordhorst et al., 1997). Since the formation of somatic embryo (SEs) was observed from colonies of single-cell origin, SE formation has been taken as evidence of the totipotency of plant cells (Steward et al., 1964; Steward et al., 1958). Although SEs were shown to share common morphological

and physiological features with zygotic embryos during their development (Dodeman et al., 1997; Zimmerman, 1993), it is not known how somatic cells acquire the competency to form SEs and how the competent cells decide when to initiate the SE-formation program. In recent decades, several transcription factors such as *WUSCHEL* (*WUS*), *LEAFY COTYLEDON 1* and *2* (*LEC1* and *LEC2*), *BABY BOOM* (*BBM*), *AGAMOUS-LIKE 15* (*AGL15*), and *PLETHORA5* (*PLT5*) have been shown to enhance SE formation when overexpressed (Boutilier et al., 2002; Harding et al., 2003; Lotan et al., 1998; Stone et al., 2001; Tsuwamoto et al., 2010; Zuo et al., 2002). Some epigenetic regulators, such as Polycomb Repressive Complex 2 (PRC2) and histone deacetylases (HDAs) have been also implicated in SE formation (Makarevich et al., 2006; Mozgova et al., 2017; Tanaka et al., 2008). However, the entire molecular framework of SE initiation is still far from understood.

The feasibility of somatic embryogenesis differs widely depending on the type of tissue and species. In carrot, a model plant for SE induction, SE formation has been observed in various types of tissues, such as stems, leaves, and shoot apices (Kamada et al., 1989; Nishiwaki et al., 2000). In *Arabidopsis thaliana*, however, only a limited number of tissues have been shown to form SEs, despite its huge advantages as a model system in which the molecular mechanisms of formation and maintenance of different

meristems and embryogenesis have been extensively studied, and large amounts of genetic tools and genome information are available. The most commonly used tissue source for inducing SEs in *A. thaliana* is zygotic embryos taken from siliques, which can be directly or indirectly (through embryogenic callus) induced to form SE (Gaj, 2001; Ikeda-Iwai et al., 2002; Sangwan et al., 1992; Su et al., 2009; Wu et al., 1992). Several studies have described the expression patterns of marker genes and transcriptome changes in embryo-derived SE induction systems (Gliwicka et al., 2013; Kurczynska et al., 2007; Su et al., 2015; Su et al., 2009; Wickramasuriya and Dunwell, 2015). Other types of tissues reported to form SEs in *A. thaliana* are leaf cell suspension cultures (Luo and Koop, 1997; Oneill and Mathias, 1993) and shoot apex and floral bud explants (Ikeda-Iwai et al., 2003). However, the former does not complete SE formation, ceasing development at the early globular stage (Luo and Koop, 1997). In the latter tissues, SEs can be successfully induced and grown into young plantlets, although the SE-formation rate is not high (Ikeda-Iwai et al., 2003). In this system, SEs and callus tissue are induced in the explants by application of osmotic stress and subsequent culture on media containing the auxin analog 2,4-dichlorophenoxyacetate (2,4-D). When SEs are formed from shoot apices, the cells dynamically change their fate from shoot to embryo, which demonstrates the plasticity of plants more clearly than the SE

induction from zygotic embryos described above. However, it remains completely unknown which cells of the shoot apex give rise to an embryo and how the morphology and gene expression of those cells change during SE induction.

Here we characterize SE formation from shoot apices by establishing experimental systems for time-lapse observation of explants and selection of SE-forming explants at the early stage of SE induction. Through the observation of several fluorescent markers, including hormone-response genes, apical meristem genes, and embryo-related genes, we show that SEs arise from the base of the leaf primordium (LP) beside the shoot apical meristem (SAM), where auxin accumulation, the formation of shoot-root polarity and transient expansion of SAM gene expression are observed at the same time. These events take place prior to callus formation, suggesting that LP cells directly convert their fate and initiate SEs without going through callus formation, while the cells surrounding the SE form callus in parallel. By transcriptome profiling of SE-forming and non-SE-forming explants (sorted by the expression pattern of an embryonic reporter at the initial stage of SE induction), we show that SE-forming explants possess a mixed identity (SAM, root and embryo) at the time of SE specification. Only a limited number of embryonic genes and root genes are enriched in SE-forming explants compared with non-SE-forming explants, suggesting that the

difference between these two explants is very subtle, but may determine the SE-formation fate.

2. Materials and Methods

2.1. Plant Materials

The reporter lines *pPIN1::PIN1-GFP* (Grieneisen et al., 2007), *pDR5rev::3XVENUS-N7/pPIN1::PIN1-GFP* (Kareem et al., 2015), *pDRN::erGFP* (Cole et al., 2009), and *pLEC1::LEC1-GFP* (Li et al., 2014) of *A. thaliana* have been described before. The generation of the *pCLV3::dsRed-N7* (Prunet et al., 2017), *pTCSn::tdTomato-N7*, *pWOX2::NLS-YFPx3* and *pWUS::dsRed-N7/pWOX5::GFPer* reporters is described below. The *pWOX5::GFPer* plants were in the Wassilewskija (Ws) background and the rest were in the Col-0 background. Seeds were surface-sterilized, kept in a cold chamber (4°C) for 1–2 nights, and plated on MGRL medium (Fujiwara et al., 1992). Plants were grown under a long-day (16 h light/8 h darkness) photoperiod.

2.2. Generation of reporter lines

The line *pCLV3::dsRed-N7* was kindly provided by Prof. E. M. Meyerowitz. The *pCLV3::dsRed-N7* reporter constructed as follows. The *CLV3* promoter was PCR

amplified from Col-0 genomic DNA staring 3.9 kb upstream of the initiating ATG for the *CLV3* cDNA. The endogenous *CLV3* 3'UTR regulatory region was PCR amplified from Col-0 genomic DNA containing 1.3 kb of DNA sequence starting at the stop codon for the *CLV3* cDNA. These fragments where subcloned into pBJ36 vector sequentially and a gateway conversion cassette was inserted between the *CLV3* promoter and 3'UTR. This cassette was then subcloned into the pMOA33 vector (Kanamycin resistance in plants) (Barrell and Conner, 2006). A version of dsRed containing the nuclear localization sequence N7 (Cutler et al., 2000) (dsRed-N7) was then recombined into this destination vector using LR clonase II (Invitrogen).

The synthetic cytokinin *pTCSn::tdTomato-N7* constructed was subcloned from the plasmid described in Zurcher et al. 2013 (Zurcher et al., 2013). The synthetic promoter containing the 35S promoter was subcloned into the pBJ36 plasmid and a gateway conversion cassette was inserted between the *TCSn* synthetic promoter and an OCS terminator. This cassette was then subcloned into pMOA34 (Hygromycin resistance in plants). To generate the *pTCSn::tdTomato-N7* a version of the tdTomato containing the nuclear localization signal N7 was recombined into the *pTCSn* destination vector using LR clonase II (Invitrogen).

The line *pWOX2::NLS-YFPx3* was kindly provided by Drs. T. Laux and M.

Ueda. The *pWOX2::NLS-YFPx3* construct was generated by modifying the *pWOX2::DsRed2* construct reported in (Ueda et al., 2011). Briefly, the *NLS-YFPx3* sequence was inserted between the *WOX2* genomic fragments of the upstream region (6959 bp upstream of the ATG start codon and 440 bp of the entire first intron) and the downstream region (1668 bp downstream of the stop codon), and the resulting sequence was cloned into a binary vector, pBarMAP (Ueda et al., 2011). Wild-type (Col-0) plants were transformed and transgenic plants were selected for Basta resistance.

The line *pWUS::dsRed-N7* was generated by agrobacterium-mediated transformation of wild-type Columbia (Col-0) plants using the *pWUS::dsRed-N7*/*PZP222* plasmid (Gordon et al., 2007). *pWUS::dsRed-N7/pWOX5::GFPer* was generated by crossing *pWUS::dsRed-N7* (described above) and *pWOX5::GFPer* (Blilou et al., 2005) plants.

2.3. Induction of somatic embryos

Induction of SE was carried out following Ikeda-Iwai et al. (Ikeda-Iwai et al., 2003) with some modifications. Shoot apex explants (about 1 mm in length) were excised from seedlings at 4 days after sowing (4DAS). For normal SE induction, both cotyledons were removed by cutting off the cotyledonary petioles. For the microscopic observation of SE induction, only one cotyledon was removed, and the explant was

plated on the medium with the abaxial side of the other cotyledon down. The explants were cultured on stress medium containing Gamborg's B-5 medium (Wako) with 20 g/l sucrose, 1× Gamborg's vitamin solution (Sigma), 0.7 M of mannitol (Wako), and 0.8% agar (Wako), with the pH adjusted to 5.7 using 1.0 M KOH. After 6 h of stress treatment, the explants were washed with B5 liquid medium, containing Gamborg's B-5 medium with 20 g/l sucrose and 1× Gamborg's vitamin solution with the pH adjusted to 5.7 using 1.0 M KOH. Then, the explants were transferred to E4.5 medium, containing Gamborg's B-5 medium with 20 g/l sucrose, 1× Gamborg's vitamin solution, 4.5 μM 2,4-D (Sigma), and 0.8% agar, with the pH adjusted to 5.7 using 1.0 M KOH. The explants were cultured at 25°C under continuous light (65 μmol photons m^{-2} s^{-1}). After 5–14 days of culture on E4.5 medium, approximately 20% of explants formed embryonic structures.

2.4. Sudan Red staining

The explants were assessed for Sudan Red staining at 7–12 days after stress application. The staining was performed with Sudan Red 7B (Santa Cruz Biotechnology) according to a previously described protocol (Aichinger et al., 2009; Bouyer et al., 2011). The explants were dehydrated through an isopropanol series (20%, 40%, 60%), and incubated for 1 h with 0.5% Sudan Red 7B solution in 60% isopropanol (Bouyer et al.,

2011). The explants were hydrated through the same series in reverse and washed three times with water (Aichinger et al., 2009). For seed staining, seeds were incubated in 10% commercial bleach and 0.01% (w/v) Triton X-100 for 24 h prior to Sudan Red staining (Beisson et al., 2007). Samples were observed with a stereomicroscope equipped with a digital camera (DP72, Olympus, http://www.olympus-ims.com/).

2.5. Microscopic imaging

Time-lapse imaging of the shoot apex explants was performed from day 1 to day 5 on E4.5 medium using an Olympus FVMPE-RS multiphoton microscope with a UPlanSApo 20× (N.A. = 0.75, WD = 0.6 mm) dry objective lens to avoid contamination caused by immersing the samples in water. Single time-point imaging of the explants at day 3 was performed using the same microscopic system with a XLPLN 25× WMP2 (N.A. = 1.05, WD = 2.00 mm) water immersion objective lens (Olympus), and the explants were stained with 100 μg/mL propidium iodide (PI) (Sigma) for 4 min before imaging. To detect GFP or VENUS or YFP together with autofluorescence or RFP signals, the laser was tuned to 920 nm (for GFP, VENUS, and YFP) with a fixed wavelength of 1040 nm (for autofluorescence or RFP). Imaging was carried out with the non-sequential scan setting. To detect signals of autofluorescence or GFP in combination with tdTomato, dsRed or PI, the laser was tuned to 920 nm (for autofluorescence or GFP) with a fixed

wavelength of 1040 nm (for tdTomato, dsRed or PI). Imaging was carried out with the sequential scan setting. All light was reflected by a FV30-SDM-M mirror. The signals were collected using a FV30-FGR filter mounted in front of gallium arsenide phosphide photomultiplier tubes (GaAsP-PMT). The Z-stacks were reconstructed into a projection view using the OLYMPUS FV30S-SW software. Five to ten samples each were imaged for SE- and non-SE-forming explants in each marker line to confirm that the observed patterns were representative of the respective markers.

2.6. RNA-seq

Shoot apex explants were excised from *pWOX2::NLS-YFPx3* plants at 4DAS. The explants were collected before and after stress application (named Shoot apex and Stress). At day 3 and day 5 on E4.5 medium, the explants were sorted based on the presence or absence of clear *pWOX2::NLS-YFPx3* signals with nuclear localization and collected (named day3 positive, day3 negative, day5 positive, and day5 negative). Total RNA was isolated from the collected explants using PureLink Plant RNA Reagent (Invitrogen). Then, 1000 ng of the RNA was used to construct transcriptome libraries according to the instructions for TruSeq RNA Sample Preparation v.2 (Illumina). The libraries were pooled and 36–86-bp single-read sequences were obtained with a NextSeq 500 sequencer (Illumina). Three independent biological replicates were

analyzed for each genotype.

2.7. RNA-seq data analysis

The quality-filtered reads were mapped onto cDNA sequences of annotated genes and other transcripts of TAIR10 using Bowtie (Langmead et al., 2009) with the parameters -all -best -strara. SE-enriched genes were identified in R using the R package edgeR (Robinson et al., 2010), treating biological triplicates as paired samples. Genes with a *p*-value < 0.05 and FC > 1.5 in each comparison were identified as SE-enriched genes. Z-scores and heatmaps were generated with the R packages gplots and genefilter.

2.8. Real time qRT-PCR

Sample preparation and RNA extraction were performed as described above (2.6. RNA-seq). Then, 100 ng of the RNA was reverse transcribed using the Verso cDNA Synthesis Kit (Thermo Scientific), following the manufacturer's instructions. Real-time qRT-PCR was performed with Luna Universal qPCR Master Mix (NEB).

The primers used for qRT-PCR were: LEC1_RTPCR_F2, 5′-CTGGACCACGATACCATTGTT-3′; LEC1_RTPCR_R2, 5′-GTGGAGCTCCCTTCTCTCACT-3′; SMB_RTPCR_F, 5′-CTCAACAAGCTGGAACCTTGG-3′; SMB_RTPCR_R, 5′-CGGGTCCCAGTCGGATATTTC-3′; WOX2_RTPCR_F3,

5′-CTCCACAAAACCTCCCGTTTC-3′; WOX2_RTPCR_R3, 5′-ATGATGATCACTTGCTTGCTG-3′; PP2A_LEFT, 5′-GACCGGAGCCAACTAGGAC-3′; and PP2A_RIGHT, 5′-AAAACTTGGTAACTTTTCCAGCA-3′. The primer sequences of LEC1 and PP2A primers were described previously (Ginglinger et al., 2013; Ledwon and Gaj, 2011).

The Thermal Cycler Dice® Real Time System III was used for the detection and relative quantification of gene expression. The qPCR cycling conditions were: 95°C for 60 s, [95°C for 15 s, 60°C for 30 s] (40 cycles), followed by dissociation curve analysis (60–95°C) to confirm primer specificity. PP2A was used as a reference gene.

3. Results

3.1. Characteristics of callus formed from shoot apex explants and SE-formation rate

Because the efficiency of SE induction is highly variable depending on the experimental conditions, such as the developmental stage of the tissue source and the length of stress application, we first reproduced the SE-induction assay established by Ikeda-Iwai *et al.* (Ikeda-Iwai et al., 2003) and developed a system for time-lapse microscopic observation of SE initiation. As reported by Ikeda-Iwai *et al.* (Ikeda-Iwai et al., 2003), shoot apex explants were excised from young seedlings, kept on stress medium containing 0.7 M

mannitol for 6 h, and then transferred to E4.5 medium containing 4.5 μM of the non-transportable auxin analog 2,4-D (Fig. 1A). For standard induction, both cotyledonary petioles were cut off from the shoot apex explant. For microscopic observation, we removed one cotyledon from the shoot apex explant to expose the SAM and cultured the explants with the abaxial side of the other cotyledon down, which enabled us to observe the reporters in the SE initiation regions and to image the samples with the same angle as the previous observation. Time-lapse imaging was carried out on days 1–5 on E4.5 medium (SE induction).

We first observed the tissue morphology of the explants at the stages when SE structures were clearly apparent if they were successfully formed. Through careful observation, we found that two types of callus were formed on the explants in the SE-induction system: smooth-surface callus and rough-surface callus (here we designate these calli SSC and RSC). SSC consisted of small proliferative cells and the tissue surface appeared smooth and watery (Fig. 1B, C). Conversely, RSC consisted of large hairy cells and the tissue surface appeared rough and dry (Fig. 1D). Almost all SE structures were formed in SSC (Fig. 1B), which was consistent with a previous report in which SE structures were observed on the surface of small watery callus (Ikeda-Iwai et al., 2003). Some of the explants died, which might have been caused by osmotic and

2,4-D stress (Fig. 1E). The ratio of SSC- and SE-forming explants decreased as the tissue source (the seedlings) aged from 4DAS to 7DAS (data not shown). Instead, RSC was more likely to be formed in explants derived from older seedlings. The 4DAS stage was optimal among the stages tested in our experiment, and gave a 20% (± 3.33% s.d., n = 90 explants) SE-formation ratio (Fig. 1F). SEs were never formed in explants derived from 7DAS seedlings, all of which formed RSC. Thus, 4DAS seedlings were used for further investigation. The changes in the SE formation rate observed in this study were comparable to those reported in (Ikeda-Iwai et al., 2003), although the optimal timing of explant excision in their study was 5DAS, which might have been because their growth conditions resulted in the seedlings growing slower.

We next performed time-lapse observation of the explants during SE induction (Fig. 1G). The cells in the central region of the explants around the SAM and the first and second true leaves proliferated and formed callus, which was first apparent at day 5 of SE induction. In particular, part of the SAM region between two enlarged leaves bulged out at day 5, and then grew larger and eventually formed a SE structure at day 7 (Fig. 1G, arrowheads). We confirmed that the induced structure was embryonic tissue by staining with Sudan Red 7B, a stain for tissue containing triacylglycerol, which is characteristic to embryos (Fig. 1H). Only faint stains were observed in RSC and the

hypocotyls of untreated seedlings, which did not give rise to SEs. Taken together, these data indicated that the cells of SAM regions in young seedlings at a specific stage were competent to form SEs, and that the fate change of the explant tissue from shoot meristem to embryonic tissue occurred directly, or indirectly through callus tissue, before day 5 of SE induction.

3.2. Distribution patterns of hormone responses and SE formation

To examine the correlation between SE initiation and the phytohormone distribution in the shoot apex explants, we observed the expression patterns of three phytohormone-related reporters upon SE induction. We first analyzed the polar auxin distribution using *pPIN1::PIN1-GFP* (Grieneisen et al., 2007) to visualize the localization of the auxin efflux carrier *PIN-FORMED 1* (*PIN1*), and *pDR5rev::3XVENUS-N7* to visualize the auxin response of the tissues (Kareem et al., 2015; Ulmasov et al., 1997). *PIN1* is involved in various aspects of plant development by setting the directional auxin flow (Petrasek and Friml, 2009). During embryogenesis, *PIN1* is expressed in the upper apical region of globular-stage embryos and the tip of the cotyledon and vasculature in heart-stage embryos (Szakonyi and Byrne, 2011). The expression of the *DR5* reporter is localized in the tip of cotyledon and hypophysis in the embryo (Friml et al., 2003). Previous studies on embryo-derived SE induction systems

showed that SEs initiate from the edge regions of the callus, where auxin accumulates and forms gradients, which was visualized using these reporters: the polar localization of *PIN1* and high-low expression of the *DR5* reporter (Su et al., 2015; Su et al., 2009). In the shoot apex explants, *PIN1* was localized in the regions of the SAM and LP (Fig. 2A). *PIN1* expression was maintained in the bulging region in the center of SE-forming explants (Fig. 2A, yellow arrows), but disappeared from the central region after day 3 in non-SE-forming explants (Fig. 2A, red arrows), suggesting that auxin transport is enhanced in the SAM or LP, which then actively proliferates and gives rise to a SE. The *DR5* reporter was also expressed in the central region of the SE-induced explants (Fig. 2B, yellow arrows), but not in the non-SE-forming explants (Fig. 2B, red arrows), suggesting that the auxin response is increased in the SE-forming region. Therefore, consistent with embryo-derived SE initiation, SE structures arise from the auxin accumulation region in shoot-derived SE induction, which is in the SAM or LP region in this case.

Next, we examined *pTCSn::tdTomato-N7* to visualize the cytokinin response. The *TCS* reporter is expressed in suspensor cells during embryogenesis (Wolters et al., 2011). In the shoot apex explants, the *TCS* reporter was hardly detected at days 1–3. Its expression increased all over the explants after day 4, but was excluded from the whole

SE-forming region at day 5 (Fig. 2C, yellow arrow), indicating that the cytokinin response is decreased in the SE-forming region at this point. We also observed a reporter for *WUSCHEL RELATED HOMEOBOX 8* (*WOX8*), which marks the suspensor region of the embryo (Ueda et al., 2011). We detected only a tiny signal of the reporter in the SE-forming region, but it was hard to tell whether the suspensor tissue was very small or was formed deeply inside the tissue, preventing a large portion of the signal from being detected (data not shown).

3.3. Expression patterns of shoot and root stem cell niche markers and SE formation

To investigate spatiotemporal stem cell niche formation in the SE, we next observed markers of shoot and root apical meristems. The first marker line contained *pWUS::dsRed-N7* for the homeobox gene *WUSCHEL* (Gordon et al., 2007) and *pWOX5::GFP-er* for *WUSCHEL-RELATED HOMEOBOX-5* (*WOX5*) (Blilou et al., 2005). These genes are expressed in the organizer center (OC) of the SAM and the quiescent center (QC) of the root apical meristem, respectively. Both genes regulate the specification and the maintenance of the stem cells surrounding the OC or QC region (Laux et al., 1996; Sarkar et al., 2007), and start to be expressed in the embryo: *WUS* expression begins in the four apical inner cells of embryos at the 16-cell stage and *WOX5* expression in the hypophysis in early globular-stage embryos (Mayer et al.,

1998; vandenBerg et al., 1997). Overexpression of the *WUS* protein causes a vegetative-to-embryonic fate change leading to SE formation (Zuo et al., 2002). In embryo-derived SE formation, *WUS* and *WOX5* reporter signals nearly overlap, and are then located adjacent each to other at the initial stage, which determines the embryonic shoot-root axis (Su et al., 2015). In the shoot apex explants, SEs were also formed in the regions in which both markers were expressed next to each other. The *WUS* expression in the SAM region slightly and transiently increased on the apical side at day 2 and then decreased afterwards (Fig. 3A). On day 3, *WOX5* expression was detected just below the region of *WUS* expression (Fig. 3A, b); this pattern was not observed in non-SE-forming explants (Fig. S1A). Therefore, our observations suggested that shoot-root polarity is established at this stage, and may enable the tissue to develop into a SE. The expression of the *WUS* reporter was detected in the callus region beneath the SE (Fig. 3A, d), suggesting that the callus tissue might have SAM-like characteristics.

The second marker line was *pCLV3::dsRed-N7* for the precursor of a secreted signal peptide *CLAVATA3*, which is expressed in the stem cells harbored in the central zone (CZ) of the SAM (Wang and Fiers, 2010). The *CLV3*-expressing cells in the CZ did not proliferate and *CLV3* expression gradually decreased in the shoot apex explants upon SE induction (Fig. 3A). Instead, the surrounding cells in the peripheral zone (PZ)

of the SAM or the third and fourth LPs seemed to proliferate and protrude, suggesting that the SE might be formed from these cell regions (Fig. 3A, c).

The third marker line was *pDRN::erGFP* for the AP2 transcription factor, *DORNRÖSCHEN* (*DRN*) (also known as *ENHANCER OF SHOOT REGENERATION1*; *ESR1*), which is strongly expressed in LP and weakly in the whole SAM in young seedlings. *DRN* expression is detected all through embryonic development from the four-cell stage, and localizes to the apical cell tiers at the transition stage, and then to the lobes of developing cotyledons, before finally being confined to the SAM (Chandler et al., 2007; Kirch et al., 2003). Upon SE induction, *DRN* expression expanded from the SAM to the base of the first and second leaves at day 1 and day 2 (Fig. 3B). The *DRN* reporter was strongly expressed over the whole SAM region in SE-forming explants at day 2 (Fig. 3B, e), but was excluded from the SAM in non-SE-forming explants at this stage (Fig. S1B). The signals disappeared from the regions of the PZ or the third and fourth LP at day 3 (Fig. 3B, f), from which SE structures formed (Fig. 3B, g and h). Analogously to *WUS*, *DRN* expression was detected in the callus region beneath the SE at day 5 (Fig. 3B). Taken together, these results suggest that, upon SE induction, *WUS* and *DRN* are upregulated in the SAM at day 2, followed by the establishment of shoot-root polarity at the base of the original SAM region at day 3, and the PZ or LP

regions may form a SE.

3.4. Expression pattern of embryonic markers and selection of SE-forming explants

To determine when the shoot explant acquires the embryonic trait during SE induction, we observed the embryonic markers *pLEC1::LEC1-GFP* (Li et al., 2014) and *pWOX2::NLS-YFP* in the explants. *LEAFY COTYLEDON1* (*LEC1*) is a central regulator of seed development, and marks zygotic embryos during normal development (Lotan et al., 1998). *WUSCHEL RELATED HOMEOBOX 2* (*WOX2*) plays a role in initiating shoot meristem stem cells in embryos (Zhang et al., 2017). Its expression starts in the fertilized egg and is localized in the apical half of the embryo after asymmetric cell division (Ueda et al., 2011). *LEC1* overexpression was previously reported to induce SE formation from vegetative tissues (Lotan et al., 1998). In European larch (*Larix decidua*), *LdLEC1* and *LdWOX2* are abundantly expressed in both zygotic embryos and SEs (Rupps et al., 2016). We observed strong and clear expression of *pLEC1::LEC1-GFP* and *pWOX2::NLS-YFP* in the induced SE structures (Fig. 4A), whereas their signals were absent from the non-SE-forming explants all through the SE induction period (Fig. S2), demonstrating that the SE structures acquired the embryonic trait and the tissue fate was changed from shoot apex to embryo. Both markers were switched on at day 3 of SE induction in the regions of PZ or the third or fourth LP,

suggesting that the SE might arise from these cells.

We next investigated whether the explants eventually formed SEs once they expressed embryonic markers at day 3. As the initial dim expression of the *WOX2* reporter was easier to detect than that of the *LEC1* reporter because of its nuclear localization, we sorted the explants according to the presence or absence of *WOX2* reporter expression at day 3 (Fig. 4B) and evaluated their SE formation by Sudan Red staining at a later stage. The explants expressing the *WOX2* reporter with clear nuclear localization formed SEs at a high ratio (74%, n = 54), while the explants lacking *WOX2* expression hardly formed SEs (4%, n = 93), suggesting that embryonic fate commitment took place by day 3 and rarely changed afterwards. These findings allow us to distinguish SE-forming explants from non-SE-forming explants at a high ratio at the early stage of SE induction before SE structures are anatomically apparent.

3.5. Tissue origin of SE formation

The results of time-lapse observation of various reporter lines described above suggested that SE fate specification takes place at day 3 of SE induction and that a SE may arise from cells in the PZ in the SAM or the LP. To determine whether the PZ or LP gives rise to the SE, we observed the reporters with PI counterstaining at day 3 using a water immersion lens to visualize tissue morphology at higher resolution, whereas for

the time-lapse observation described above, the samples were observed without PI staining in dry conditions to avoid contamination. We found that the *WOX2* reporter was expressed in the base of the third or fourth LP (Fig. 5A). The cells in the boundary region and the adaxial side of the LP expressed the *WOX2* reporter and appeared to proliferate. PIN1 localization and an adjacent expression pattern for the *WUS/WOX5* reporters were also detected in a similar region of the explants (Fig. 5B–C'). Therefore, the SE arises from the base of a LP just beside the SAM, where the auxin gradient and shoot-root polarity are formed. Callus tissue was not yet formed in this area of the explants, but was clearly apparent at day 5 (Fig. 1G), suggesting that SE specification does not take place in callus-forming cells.

3.6. Changes of the molecular identity of shoot apex explants during SE induction

To determine how the molecular identity of the explants changes at a genome-wide scale in the event of SE induction and subsequent SE formation, we next analyzed the transcriptome changes of the explants during SE induction by RNA-sequencing. We examined the explants before and after stress application (named Shoot apex and Stress, respectively), and SE-forming and non-SE-forming explants at days 3 and 5 of SE induction, sorted by the presence or absence of the *WOX2* reporter signal with nuclear localization (named day-3-positive, day-3-negative, day-5-positive, and

day-5-negative-explants, respectively) (Fig. 6A). We first compared the expression intensities of key developmental genes for embryos, and shoot and root meristems between stages during SE induction (Fig. 6B–D). As shown in Fig. 6B, several key genes for embryonic development, such as *LEC1*, *LEC2*, *ABSCISIC ACID-INSENSITIVE3* (*ABI3*) and *FUSCA3* (*FUS3*) (Jia et al., 2013; Jia et al., 2014), started to be expressed at higher levels in day-3-positive explants than in day-3-negative explants. The difference between positive and negative explants was more obvious at day 5. The expression of all the listed genes except *WOX2* was greater in day-5-positive explants than in day-5-negative explants, indicating that the day-5-positive explants had developed embryos, while the others had not. Notably, *WOX2* expression was even higher in the shoot explants before SE induction because of its low expression level in the embryo compared to the plant (Chung et al., 2016). We confirmed that *WOX2* expression was higher in positive explants than in negative explants on both days 3 and 5 (Fig. S3). We also performed qRT-PCR and confirmed that *LEC1* and *WOX2* expression was high in positive explants compared with negative explants after day 3 (Fig. S7A, C and C'). Thus, the SE-forming and non-SE-forming explants were successfully sorted for transcriptome analysis. Consistent with the imaging data, this result suggests that the SE-forming explants initiate the embryonic developmental

program at day 3, which continues thereafter without changing the cell fate.

The key developmental genes for the shoot meristem *CLV3*, *UNUSUAL FLORAL ORGANS* (*UFO*), and *CUP-SHAPED COTYLEDON 3* (*CUC3*), which are expressed in the CZ and PZ of the shoot meristem and the boundary region between the shoot meristem and lateral organs, respectively, were downregulated at the SE induction stages (day 3 and day 5) compared with shoot explants just before and after stress application (Fig. 6B), suggesting the partial loss of the normal shoot trait attributed to the expression of these genes during SE induction. In the meantime, *WUS*, *DRN*, *DRN-like* and *CUC1*, which are expressed in the OC, CZ and boundary region, respectively, were transiently upregulated at the initial stage of SE induction (day 3), which may contribute to provide the stemness to the cells so that they can acquire the embryonic trait and divide into a SE. The downregulation of *CLV3* during the SE induction process and the transient upregulation of *WUS* at the SE initiation stage detected here in RNAseq analysis were consistent with the imaging data (Fig. 3A). As a whole, both the shoot and root meristem key genes showed expression changes depending on the explant stage, but only small difference between positive and negative explants at either day 3 or day 5 (Fig. 6C and D). We also confirmed this finding by examining many data sets from various root tissue types (data not shown). Therefore,

SE-forming and non-SE-forming explants mostly shared the same tissue traits except for the initiation of the embryonic developmental program, which was triggered by a limited number of embryonic genes. This was consistent with the result that only a small number of genes were identified as SE-enriched genes by comparison of SE-forming and non-SE-forming explants at each stage (FC > 1.5, $p < 0.05$) (Fig. 7A).

3.7. Root-shoot-embryo mixed character of SE-forming explants

Next, we focused on the differentially expressed genes between SE-forming and non-SE-forming explants. By comparing SE-forming and non-SE-forming explants at each stage (FC > 1.5, $p < 0.05$), the genes enriched in SE-forming explants (SE-enriched genes) were identified, including 73 genes at day 3 and 159 genes at day 5. Given the total number of genes in *A. thaliana* and the clear difference in phenotype between the explants, these numbers are relatively small. Among them, only 11 genes overlapped between the two stages, indicating a dynamic change of the determinant trait for SE-formation between these two stages (Fig. 7A).

We investigated the expression of the SE-enriched genes in various tissue types in plant development using previously reported expression data sets (Belmonte et al., 2013; Birnbaum et al., 2003) (Fig. 7B and C). All gene data sets were normalized to the expression intensity of *PP2A* (AT1G69960). We also normalized the data sets to *ACT7*

(AT5G09810) and *UBI10* (AT4G05320) and performed the same analysis to confirm that the results showed similar tendencies regardless of the gene used for normalization (Fig. S4 and S5). The SE-enriched genes at day 3 were preferentially expressed in root tissues. In particular, a large cluster of genes was highly abundant in the lateral root cap (LRC) at the root tip (Fig. 7B). Conversely, the SE-enriched genes at day 5 were rarely expressed in root tissues (Fig. 7C). However, the SE-enriched genes at day 3 highly expressed in the root tip LRC were even more upregulated in both SE-forming and non-SE-forming explants at day 5 (Fig. 7D), but were not identified as SE-enriched genes at day 5 because the difference between SE-forming and non-SE-forming explants was smaller at this stage. Thus, although these LRC genes are eventually highly expressed in both explants, they start to be expressed in SE-forming explants earlier than in non-forming explants, which may be important for SE competency. We performed qRT-PCR for the LRC gene *SOMBRERO* (*SMB*) (Fendrych et al., 2014), which was included in the SE-enriched genes at day 3, and confirmed that the *SMB* expression level was higher in positive explants than in negative explants at day 3 but not at day 5 (Fig. S7B). We also compared the expression intensity of LRC-expressed genes (Brady et al., 2007) between stages during SE induction, and found that only some LRC genes were upregulated upon SE induction (Fig. S6), suggesting that the

explant tissue as a whole is not similar to the LRC but shares some trait with it. The SE-enriched genes at day 5 were preferentially expressed in the tissues of mature green embryos in seeds (Fig. 7C). Therefore, the SEs formed in the explants might have developed into mature green embryos by day 5.

Taking all the RNA-seq results together (Figs. 6 and 7), SAM genes such as *WUS* and *DRN*, embryonic genes, and genes expressed in the root, especially in the LRC, are expressed together prior to or at the same time as the determination of SE formation in the explants.

4. Discussion

4.1. Characterization of SE formation in shoot apex explants

SE induction from the shoot apex demonstrates the remarkable developmental plasticity of plants and is a good system to study the mechanisms of cellular reprogramming of somatic cells in multicellular organisms. However, basic information about this phenomenon, such as the cellular origin of SEs and the morphological and transcriptome changes of the cells during SE induction, is lacking. In this study, we characterized SE formation from the shoot apex by time-lapse observation of tissue morphology and fluorescent reporters and by transcriptome profiling of SE-forming and non-forming explants prior to the appearance of SE structures.

The time-lapse observation of tissue morphology and fluorescent reporters revealed when and where the SE arises in the shoot apex. Unlike SE formation from embryo-derived callus, shoot-derived SEs form at a specific position in the explants. The cells at the base of the LP switch on embryonic markers and proliferate, where an auxin gradient and shoot-root polarity appear to be formed at the same time (day 3 of SE induction), prior to callus formation (day 5). Analogous patterns of an auxin gradient and shoot-root polarity have been observed when embryo-derived SEs are initiated (Su et al., 2015; Su et al., 2009). This suggests that the cells of the LP reprogram themselves and directly give rise to a SE without the intermediate process of callus formation, while the cells surrounding the SE and in the leaves in the SE-forming explants might proliferate in parallel and form SSC callus at later stages.

For the transcriptome analysis, we sorted the explants according to their expression of the *WOX2* reporter at the initial stage of SE induction. To screen for SE-associated genes, previous studies have used the following tissues as non-SE-forming tissues for comparisons in transcriptome analysis; different types of tissues, the same tissues under different treatments or at different stages, or the same tissues under the same treatment in different genotype backgrounds (Gliwicka et al., 2013; Low et al., 2008; Thibaud-Nissen et al., 2003; Wickramasuriya and Dunwell,

2015). However, these approaches might select genes that are not directly involved in SE formation but show different responses to the cultural treatment depending on the tissue type or genotype. In our approach, the tissue source, genetic background, cultural conditions, and stage are all constant between SE-forming and non-SE-forming explants. Thus, our approach may enable us to focus on the gene expression changes associated with the determination of SE fate. Indeed, our results revealed subtle transcriptome differences between SE-forming and non-SE-forming explants.

Taken together, our characterization data from time-lapse observation and transcriptome analysis narrow down the time, place and transcripts to focus on for further studies on the mechanisms that regulate the fate conversion and SE-initiation program in shoot apex explants.

4.2. Mixed identity of SE-forming explants

In the embryo-derived SE system, embryonic genes are expressed in the explants all through the cultural treatment (Su et al., 2009). In shoot apex explants, our imaging and transcriptome data showed that the expression of several key embryo genes started at day 3 of SE induction, and that other key genes joined to be expressed at day 5, suggesting that SE specification takes place by day 3 and more and more embryonic developmental programs operate afterwards. Conversely, several key genes for the shoot

meristem, such as *CLV3* and *UFO*, were downregulated at day 3, suggesting the partial loss of the normal shoot trait attributed to these genes by this time. Therefore, our data clearly demonstrated the fate conversion of SE-forming explants from shoot to embryo during SE induction. Meanwhile, several other SAM genes, such as *WUS* and *DRN*, were transiently upregulated at day 3 in both SE-forming and non-SE-forming explants, suggesting that the expression changes of SAM genes in SE induction are not a determinant factor for SE specification but might be required for the cells to acquire the competence to form SEs.

As for the differentially expressed genes between SE-forming and non-SE-forming explants, a relatively small number of genes were identified as SE-enriched genes at day 3 of SE induction, including many genes highly expressed in the root tip LRC. Although these LRC genes were eventually highly expressed in both explants, their expression began earlier in SE-forming explants than in non-forming explants, which may be important for SE specification. Thus, the SE-forming explants expressed shoot genes, root genes and embryonic genes at the moment of SE specification (Fig. 8A). It is possible that the mixed expression of genes associated with various tissue types from shoots to roots during some specific time window is essential for cells to acquire the SE fate. Once that specific stage has passed, the cells may lose

their competency and SE specification may never occur even with the expression of root genes. However, another possibility is that the expression of root genes is a result of SE initiation, as embryonic genes are already expressed at day 3. To determine whether root gene expression is upstream or downstream of SE initiation, we need to find a way to predict which explants form SEs before day 3 and analyze the transcriptome profiles at that time.

In any case, considering previous results (Gaj et al., 2005), the expression of key embryo genes at day 3 should be important for SE formation. The continuous expression of these genes may support the high efficiency of SE formation in embryo-derived callus. It remains to be determined what factors trigger the expression of embryonic genes in shoot-derived tissue; such information would provide insight into the mechanisms underlying shoot-to-embryo fate conversion.

4.3. SE formation initiates at the base of LP beside SAM in shoot apex explants

Prior studies on embryo-derived SE induction have shown that the auxin response is upregulated in the edge of embryonic callus, where a local auxin gradient is formed and *WUS* starts to be expressed in the inner layer of the gap region surrounded by a high auxin region. Subsequently, the auxin-responsive signal and *WUS* expression overlap in the top of the promeristem of the SE (Su et al., 2009). The cytokinin-responsive signal

detected using the type-A *ARR7* reporter initially overlaps with the auxin-responsive signal in the edge of the callus, and then gradually moves to the basal part of the pro-embryo and substantially overlaps with *WOX5* expression (Su et al., 2015). In correlation to the distribution patterns of hormone responses, the *WUS* and *WOX5* reporter signals nearly overlap, and then appear adjacent each other at the initial stage and determine the embryonic shoot-root axis (Su et al., 2015). Analogously to embryo-derived SE formation, we observed auxin accumulation just beside the SAM region of the shoot apex explants, where *WUS* was expressed adjacent to *WOX5* expression. The SE arose from the regions where shoot-root polarity was formed, which corresponded to the base of LP regions beside the SAM. The *LEC1* and *WOX2* embryonic reporters also started to be expressed in these regions at day 3 (Fig. 8B). The difference between embryo- and shoot-derived SE formation appears to be that *WUS* is expressed from the beginning in the original SAM tissue. In embryonic callus, an auxin gradient is first triggered by removing 2,4-D and may define the *WUS* domain. In the shoot apex explants, the location of *WUS* is already determined. However, expansion of the *WUS* domain was observed at day 2, and it was expressed slightly more on the apical side (Fig. 3b). Observation of the *PIN1* and *DR5* reporters at a finer resolution will tell us whether a local auxin gradient is formed to regulate the expansion and

repositioning of *WUS* expression on the apical side. Another contrast between the two systems is the distribution pattern of the cytokinin-responsive signal relative to *WOX5* expression. Unlike the overlap of the *ARR7* and *WOX5* reporters in embryonic callus (Su et al., 2015), the *TCS* reporter was not expressed in the *WOX5* expression domain at either day 3 or day 5 in the shoot explants. Especially at day 5, the *TCS* reporter was absent from the SEs, while *WOX5* was highly expressed (Fig. 8B). This might just be caused by the differences between the cytokinin-responsive reporters (*ARR7* and *TCS* reporters). However, another possible reason is again the presence of SAM tissue in the shoot apex. The SAM might be a source of positional information and determine the position of the root apical meristem in its opposite end without needing a cytokinin signal. In this case, how does the SAM region regulate the positioning of the root meristem in close proximity? Studying the mechanisms that release the suppression of root meristem genes in the shoot apex in normal development and its spatio-temporal regulation during SE induction will give an insight into two events observed in plant regeneration: fate conversion and the reconstruction of a stem cell niche in amputated shoots and roots.

4.4. Stress and the acquisition of competency to form SE

SE formation can be induced by various types of stress, such as osmotic stress, heavy

metal ion stress, drought stress and cold stress (Kamada et al., 1989; Nishiwaki et al., 2000). In the SE-induction system described in this study, osmotic stress was used in combination with 2,4-D treatment. Although the mechanisms by which osmotic stress initiates the SE-formation program are not yet clear, the abscisic acid (ABA) signaling pathway is probably involved. It has been reported that both osmotic stress and 2,4-D promote the ABA signaling pathway by activating ABA biosynthesis (Song, 2014; Xiong et al., 2002). In carrot, ABA application was observed to induce SEs from hypocotyl epidermal cells (Nishiwaki et al., 2000), and in *Arabidopsis* embryonic callus, SE formation was greatly perturbed by the ABA biosynthesis inhibitor, fluridone (Su et al., 2013). Therefore, the ABA signal is expected to be upregulated in shoot apex explants upon SE induction. However, ABA signal component genes were not identified as SE-enriched genes at day 3 in our study. We observed that the ABA signal was commonly upregulated in both SE-forming and non-forming explants, which were subjected to the same treatment (data not shown). Thus, the ABA signal might be important but not sufficient for the acquisition of competency to form SEs.

In addition to activating specific signaling pathways, stress application may play a role in breaking or loosening cell-cell communication. Under osmotic stress, some cells undergo substantial cell plasmolysis, plasmodesmatal rupture or cell death,

leaving the surviving cells isolated without cell-cell interactions. Characteristic cellular architectures, such as a large central nucleus, dense cytoplasm, and thick cell wall with few or no plasmodesmata, are widely observed in SEs across different original tissue types and species (Chapman et al., 2000; Verdeil et al., 2007). In fact, previous observations showed that a loss of communication between neighboring cells causes the dedifferentiation and acquisition of pluripotency in each cell. In a classical study in carrot, Steward *et al*. showed that SE formation was initiated from suspended cells, suggesting that a prime factor in the determination of SE formation or non-formation in a cell is the degree to which it has become free from the constraints imposed by its neighboring cells (Steward et al., 1964). In *A. thaliana*, it has been observed that differentiated leaf mesophyll cells undergo dedifferentiation in response to removal of the cell wall (Avivi et al., 2004; Grafi, 2004). Conversely, cells in the meristems have thin primary cell walls and are tightly connected with each other via plasmodesmata (Byrne et al., 2003; Haywood et al., 2002; Verdeil et al., 2007). Stem cells regulate the cell division of surrounding cells and maintain their stem cell identity via mobile transcription factors, signal peptides and a flow of phytohormones, which keeps the size of the meristem constant (Aichinger et al., 2012). In SE induction from the shoot apex, osmotic stress breaks the cell-cell interaction of the SAM cells resulting in expanded

expression of several shoot meristem genes at day 3, which may provide a platform for SE formation.

4.5. Stress and fate specification of the SE

Stress responses and developmental fate are tightly linked. A previous study demonstrated that cell identity regulators control both development and stress response pathways in response to environmental stress (Iyer-Pascuzzi et al., 2011), indicating that stress responses are diverse depending on the cell types of tissues. Because SE formation from the shoot apex can be induced by applying osmotic stress together with 2,4-D treatment in various species besides *Arabidopsis*, such as carnation, carrot, kidney beans and cucumber (Cabrera-Ponce et al., 2015; Ikeda-Iwai et al., 2003; Karami et al., 2006; Lou and Kako, 1995), cell identity regulators of a specific cell type in the shoot apex might regulate the molecular pathways for the response to this type of stress and for SE formation. As we observed that SEs arose from the regions of LP, we speculate that one possible cell type is LP cells and one possible cell identity regulator is *DRN*, which is reported to be strongly expressed in the LP of young seedlings, and whose expression was observed to expand all over the SAM region upon SE induction in our study. However, *DRN* alone is not sufficient for SE fate specification, as SEs do not form from whole SAM regions, indicating that additional factors are required for SE

specification. Another candidate beside *DRN* is the cell identity regulator of the root tip LRC. Small differences in the stress response among explants may cause early or late upregulation of the LRC identity regulator and its downstream cluster of LRC genes, which might result in SE specification or non-specification.

It was shown that stress responses not only depend on the cell type but also on the developmental stage (Iyer-Pascuzzi et al., 2011), which may explain why only explants excised from seedlings in a specific stage can form SEs; for example, the 4DAS seedling stage in our study. In the case of the *Arabidopsis* shoot apex, the competency to respond to stress and to form SEs was retained only in the third and fourth LPs of 4DAS seedlings, which might be related to the developmental phase of the plant, such as juvenility. It will be interesting to investigate the genes that are upregulated only in the explants of 4DAS seedlings upon SE induction.

Acknowledgements

We thank K. Boutilier for *pLEC1::LEC1-GFP* seeds, T. Laux and M. Ueda for *pWOX2::WOX2-NLS-YFPx3*, W. Werr for *DRNp::erGFP* seeds, V. A. Grieneisen for *pPIN1::PIN1-GFP* seeds, C. Ohno for the *pWUS::dsRed-N7*/*PZP222* plasmid, E. M.

Meyerowitz for *pCLV3::dsRed-N7* seeds, B. Scheres for *pWOX5::GFPer* seeds and K. Prasad for *pDR5rev::3XVENUS-N7*/*pPIN1::PIN1-GFP* seeds. We thank J. Harrison for the for critical reading and comments on the manuscript, H. Ishihara for advice and assistance on RNA-seq analysis, M. Aida, Y. Jaio and members in Matsunaga's laboratory for valuable comments and discussion. This research was supported by CREST grants from the Japan Science and Technology Agency (JPMJCR13B4) and MXT/JSPS KAKENHI (25113002, 15H05955 and 15H05962) to S.M. We thank Robbie Lewis, MSc, from Edanz Group (www.edanzediting.com/ac) for editing a draft of this manuscript.

Authors Contributions

SK and KS, Conception and design, Analysis and interpretation of data, Drafting and revising the article; SK, Acquisition of data; PT, Generation of unpublished material; TS, RNA-sequencing; SM, Revising the article

References

Aichinger, E., Kornet, N., Friedrich, T., Laux, T., 2012. Plant Stem Cell Niches, in: Merchant, S.S. (Ed.), Annual Review of Plant Biology, Vol 63. Annual Reviews, Palo Alto, pp. 615-636.

Aichinger, E., Villar, C.B.R., Farrona, S., Reyes, J.C., Hennig, L., Kohler, C., 2009.

CHD3 Proteins and Polycomb Group Proteins Antagonistically Determine Cell Identity in Arabidopsis. Plos Genetics 5, 12.

Avivi, Y., Morad, V., Ben-Meir, H., Zhao, J., Kashkush, K., Tzfira, T., Citovsky, V., Grafi, G., 2004. Reorganization of specific chromosomal domains and activation of silent genes in plant cells acquiring pluripotentiality. Developmental Dynamics 230, 12-22.

Barrell, P.J., Conner, A.J., 2006. Minimal T-DNA vectors suitable for agricultural deployment of transgenic plants. Biotechniques 41, 708-710.

Beisson, F., Li, Y.H., Bonaventure, G., Pollard, M., Ohlrogge, J.B., 2007. The acyltransferase GPAT5 is required for the synthesis of suberin in seed coat and root of Arabidopsis. Plant Cell 19, 351-368.

Belmonte, M.F., Kirkbride, R.C., Stone, S.L., Pelletier, J.M., Bui, A.Q., Yeung, E.C., Hashimoto, M., Fei, J., Harada, M., Munoz, M.D., Le, B.H., Drews, G.N., Brady, S.M., Goldberg, R.B., Harada, J.J., 2013. Comprehensive developmental profiles of gene activity in regions and subregions of the Arabidopsis seed. Proceedings of the National Academy of Sciences of the United States of America 110, E435-E444.

Birnbaum, K., Shasha, D.E., Wang, J.Y., Jung, J.W., Lambert, G.M., Galbraith, D.W., Benfey, P.N., 2003. A gene expression map of the Arabidopsis root. Science 302, 1956-1960.

Blilou, I., Xu, J., Wildwater, M., Willemsen, V., Paponov, I., Friml, J., Heidstra, R., Aida, M., Palme, K., Scheres, B., 2005. The PIN auxin efflux facilitator network controls growth and patterning in Arabidopsis roots. Nature 433, 39-44.

Boutilier, K., Offringa, R., Sharma, V.K., Kieft, H., Ouellet, T., Zhang, L.M., Hattori, J., Liu, C.M., van Lammeren, A.A.M., Miki, B.L.A., Custers, J.B.M., Campagne, M.M.V., 2002. Ectopic expression of BABY BOOM triggers a conversion from vegetative to embryonic growth. Plant Cell 14, 1737-1749.

Bouyer, D., Roudier, F., Heese, M., Andersen, E.D., Gey, D., Nowack, M.K., Goodrich, J., Renou, J.P., Grini, P.E., Colot, V., Schnittger, A., 2011. Polycomb Repressive Complex 2 Controls the Embryo-to-Seedling Phase Transition. Plos Genetics 7, 19.

Brady, S.M., Orlando, D.A., Lee, J.Y., Wang, J.Y., Koch, J., Dinneny, J.R., Mace, D., Ohler, U., Benfey, P.N., 2007. A high-resolution root spatiotemporal map reveals dominant expression patterns. Science 318, 801-806.

Byrne, M.E., Kidner, C.A., Martienssen, R.A., 2003. Plant stem cells: divergent pathways and common themes in shoots and roots. Current Opinion in Genetics & Development 13, 551-557.

Cabrera-Ponce, J.L., Lopez, L., Leon-Ramirez, C.G., Jofre-Garfias, A.E.,

Verver-y-Vargas, A., 2015. Stress induced acquisition of somatic embryogenesis in common bean Phaseolus vulgaris L. Protoplasma 252, 559-570.
Chandler, J.W., Cole, M., Flier, A., Grewe, B., Werr, W., 2007. The AP2 transcription factors DORNROSCHEN and DORNROSCHEN-LIKE redundantly control Arabidopsis embryo patterning via interaction with PHAVOLUTA. Development 134, 1653-1662.
Chapman, A., Blervacq, A.S., Vasseur, J., Hilbert, J.L., 2000. Arabinogalactan-proteins in Cichorium somatic embryogenesis: effect of beta-glucosyl Yariv reagent and epitope localisation during embryo development. Planta 211, 305-314.
Chung, K., Sakamoto, S., Mitsuda, N., Suzuki, K., Ohme-Takagi, M., Fujiwara, S., 2016. WUSCHEL-RELATED HOMEOBOX 2 is a transcriptional repressor involved in lateral organ formation and separation in Arabidopsis. Plant Biotechnology 33, 245-+.
Cole, M., Chandler, J., Weijers, D., Jacobs, B., Comelli, P., Werr, W., 2009. DORNROSCHEN is a direct target of the auxin response factor MONOPTEROS in the Arabidopsis embryo. Development 136, 1643-1651.
Cutler, S.R., Ehrhardt, D.W., Griffitts, J.S., Somerville, C.R., 2000. Random GFP :: cDNA fusions enable visualization of subcellular structures in cells of Arabidopsis at a high frequency. Proceedings of the National Academy of Sciences of the United States of America 97, 3718-3723.
Dodeman, V.L., Ducreux, G., Kreis, M., 1997. Zygotic embryogenesis versus somatic embryogenesis. Journal of Experimental Botany 48, 1493-1509.
Fendrych, M., Van Hautegem, T., Van Durme, M., Olvera-Carrillo, Y., Huysmans, M., Karimi, M., Lippens, S., Guerin, C.J., Krebs, M., Schumacher, K., Nowack, M.K., 2014. Programmed Cell Death Controlled by ANACO33/SOMBRERO Determines Root Cap Organ Size in Arabidopsis. Current Biology 24, 931-940.
Friml, J., Vieten, A., Sauer, M., Weijers, D., Schwarz, H., Hamann, T., Offringa, R., Jurgens, G., 2003. Efflux-dependent auxin gradients establish the apical-basal axis of Arabidopsis. Nature 426, 147-153.
Fujiwara, T., Hirai, M.Y., Chino, M., Komeda, Y., Naito, S., 1992. EFFECTS OF SULFUR NUTRITION ON EXPRESSION OF THE SOYBEAN SEED STORAGE PROTEIN GENES IN TRANSGENIC PETUNIA. Plant Physiology 99, 263-268.
Gaj, M.D., 2001. Direct somatic embryogenesis as a rapid and efficient system for in vitro regeneration of Arabidopsis thaliana. Plant Cell Tissue and Organ Culture 64, 39-46.
Gaj, M.D., Zhang, S.B., Harada, J.J., Lemaux, P.G., 2005. Leafy cotyledon genes are essential for induction of somatic embryogenesis of Arabidopsis. Planta 222, 977-988.

Ginglinger, J.F., Boachon, B., Hofer, R., Paetz, C., Kollner, T.G., Miesch, L., Lugan, R., Baltenweck, R., Mutterer, J., Ullmann, P., Beran, F., Claudel, P., Verstappen, F., Fischer, M.J.C., Karst, F., Bouwmeester, H., Miesch, M., Schneider, B., Gershenzon, J., Ehlting, J., Werck-Reichhart, D., 2013. Gene Coexpression Analysis Reveals Complex Metabolism of the Monoterpene Alcohol Linalool in Arabidopsis Flowers. Plant Cell 25, 4640-4657.

Gliwicka, M., Nowak, K., Balazadeh, S., Mueller-Roeber, B., Gaj, M.D., 2013. Extensive Modulation of the Transcription Factor Transcriptome during Somatic Embryogenesis in Arabidopsis thaliana. Plos One 8, 20.

Gordon, S.P., Heisler, M.G., Reddy, G.V., Ohno, C., Das, P., Meyerowitz, E.M., 2007. Pattern formation during de novo assembly of the Arabidopsis shoot meristem. Development 134, 3539-3548.

Grafi, G., 2004. How cells dedifferentiate: a lesson from plants. Developmental Biology 268, 1-6.

Grieneisen, V.A., Xu, J., Maree, A.F.M., Hogeweg, P., Scheres, B., 2007. Auxin transport is sufficient to generate a maximum and gradient guiding root growth. Nature 449, 1008-1013.

Harding, E.W., Tang, W.N., Nichols, K.W., Fernandez, D.E., Perry, S.E., 2003. Expression and maintenance of embryogenic potential is enhanced through constitutive expression of AGAMOUS-Like 15. Plant Physiology 133, 653-663.

Haywood, V., Kragler, F., Lucas, W.J., 2002. Plasmodesmata: Pathways for protein and ribonucleoprotein signaling. Plant Cell 14, S303-S325.

Ikeda-Iwai, M., Satoh, S., Kamada, H., 2002. Establishment of a reproducible tissue culture system for the induction of Arabidopsis somatic embryos. Journal of Experimental Botany 53, 1575-1580.

Ikeda-Iwai, M., Umehara, M., Satoh, S., Kamada, H., 2003. Stress-induced somatic embryogenesis in vegetative tissues of Arabidopsis thaliana. Plant Journal 34, 107-114.

Iyer-Pascuzzi, A.S., Jackson, T., Cui, H.C., Petricka, J.J., Busch, W., Tsukagoshi, H., Benfey, P.N., 2011. Cell Identity Regulators Link Development and Stress Responses in the Arabidopsis Root. Developmental Cell 21, 770-782.

Jia, H.Y., McCarty, D.R., Suzuki, M., 2013. Distinct Roles of LAFL Network Genes in Promoting the Embryonic Seedling Fate in the Absence of VAL Repression. Plant Physiology 163, 1293-1305.

Jia, H.Y., Suzuki, M., McCarty, D.R., 2014. Regulation of the seed to seedling developmental phase transition by the LAFL and VAL transcription factor networks. Wiley Interdisciplinary Reviews-Developmental Biology 3, 135-145.

Kamada, H., Kobayashi, K., Kiyosue, T., Harada, H., 1989. STRESS-INDUCED SOMATIC EMBRYOGENESIS IN CARROT AND ITS APPLICATION TO SYNTHETIC SEED PRODUCTION. In Vitro Cellular & Developmental Biology 25, 1163-1166.

Kamada, H., Ishihara, K., Saga, H., Harada, H., 1993. Induction of Somatic Embryogenesis in Carrot by Osmotic Stress. Plant Tissue Lett 10, 38-44.

Kamada, H., Tachikawa, Y., Saitou, T., Harada, H., 1994. Heat Stress Induction of Carrot Somatic Embryogenesis. Plant Tissue Cult Lett 11, 229-232.

Karami, O., Deljou, A., Esna-Ashari, M., Ostad-Ahmadi, P., 2006. Effect of sucrose concentrations on somatic embryogenesis in carnation (Dianthus caryophyllus L.). Scientia Horticulturae 110, 340-344.

Kareem, A., Durgaprasad, K., Sugimoto, K., Du, Y.J., Pulianmackal, A.J., Trivedi, Z.B., Abhayadev, P.V., Pinon, V., Meyerowitz, E.M., Scheres, B., Prasad, K., 2015. PLETHORA Genes Control Regeneration by a Two-Step Mechanism. Current Biology 25, 1017-1030.

Kirch, T., Simon, R., Grunewald, M., Werr, W., 2003. The DORNROSCHEN/ENHANCER OF SHOOT REGENERATION1 gene of Arabidopsis acts in the control of meristem cell fate and lateral organ development. Plant Cell 15, 694-705.

Kiyosue, T., Kamada, H., Harada, H., 1989. Induction of Somatic Embryogenesis by Salt Stress in Carrot. Plant Tissue Cult Lett 6, 162-164.

Kurczynska, E.U., Gaj, M.D., Ujczak, A., Mazur, E., 2007. Histological analysis of direct somatic embryogenesis in Arabidopsis thaliana (L.) Heynh. Planta 226, 619-628.

Langmead, B., Schatz, M.C., Lin, J., Pop, M., Salzberg, S.L., 2009. Searching for SNPs with cloud computing. Genome Biology 10, 10.

Laux, T., Mayer, K.F.X., Berger, J., Jurgens, G., 1996. The WUSCHEL gene is required for shoot and floral meristem integrity in Arabidopsis. Development 122, 87-96.

Ledwon, A., Gaj, M.D., 2011. LEAFY COTYLEDON1, FUSCA3 expression and auxin treatment in relation to somatic embryogenesis induction in Arabidopsis. Plant Growth Regulation 65, 157-167.

Li, H., Soriano, M., Cordewener, J., Muino, J.M., Riksen, T., Fukuoka, H., Angenent, G.C., Boutilier, K., 2014. The Histone Deacetylase Inhibitor Trichostatin A Promotes Totipotency in the Male Gametophyte. Plant Cell 26, 195-209.

Lotan, T., Ohto, M., Yee, K.M., West, M.A.L., Lo, R., Kwong, R.W., Yamagishi, K., Fischer, R.L., Goldberg, R.B., Harada, J.J., 1998. Arabidopsis LEAFY COTYLEDON1 is sufficient to induce embryo development in vegetative cells. Cell 93, 1195-1205.

Lou, H., Kako, S., 1995. ROLE OF HIGH SUGAR CONCENTRATIONS IN INDUCING SOMATIC EMBRYOGENESIS FROM CUCUMBER COTYLEDONS. Scientia Horticulturae 64, 11-20.

Low, E.T.L., Alias, H., Boon, S.H., Shariff, E.M., Tan, C.Y.A., Ooi, L.C.L., Cheah, S.C., Raha, A.R., Wan, K.L., Singh, R., 2008. Oil palm (Elaeis guineensis Jacq.) tissue culture ESTs: Identifying genes associated with callogenesis and embryogenesis. Bmc Plant Biology 8, 19.

Luo, Y.K., Koop, H.U., 1997. Somatic embryogenesis in cultured immature zygotic embryos and leaf protoplasts of Arabidopsis thaliana ecotypes. Planta 202, 387-396.

Makarevich, G., Leroy, O., Akinci, U., Schubert, D., Clarenz, O., Goodrich, J., Grossniklaus, U., Kohler, C., 2006. Different Polycomb group complexes regulate common target genes in Arabidopsis. Embo Reports 7, 947-952.

Mayer, K.F.X., Schoof, H., Haecker, A., Lenhard, M., Jurgens, G., Laux, T., 1998. Role of WUSCHEL in regulating stem cell fate in the Arabidopsis shoot meristem. Cell 95, 805-815.

Mordhorst, A.P., Toonen, M.A.J., deVries, S.C., 1997. Plant embryogenesis. Critical Reviews in Plant Sciences 16, 535-576.

Mozgova, I., Munoz-Viana, R., Hennig, L., 2017. PRC2 Represses Hormone-Induced Somatic Embryogenesis in Vegetative Tissue of Arabidopsis thaliana. Plos Genetics 13, 27.

Nishiwaki, M., Fujino, K., Koda, Y., Masuda, K., Kikuta, Y., 2000. Somatic embryogenesis induced by the simple application of abscisic acid to carrot (Daucus carota L.) seedlings in culture. Planta 211, 756-759.

Oneill, C.M., Mathias, R.J., 1993. REGENERATION OF PLANTS FROM PROTOPLASTS OF ARABIDOPSIS-THALIANA L CV COLUMBIA (C24), VIA DIRECT EMBRYOGENESIS. Journal of Experimental Botany 44, 1579-1585.

Petrasek, J., Friml, J., 2009. Auxin transport routes in plant development. Development 136, 2675-2688.

Prunet, N., Yang, W.B., Das, P., Meyerowitz, E.M., Jack, T.P., 2017. SUPERMAN prevents class B gene expression and promotes stem cell termination in the fourth whorl of Arabidopsis thaliana flowers. Proceedings of the National Academy of Sciences of the United States of America 114, 7166-7171.

Robinson, M.D., McCarthy, D.J., Smyth, G.K., 2010. edgeR: a Bioconductor package for differential expression analysis of digital gene expression data. Bioinformatics 26, 139-140.

Rupps, A., Raschke, J., Rummler, M., Linke, B., Zoglauer, K., 2016. Identification of

putative homologs of Larix decidua to BABYBOOM (BBM), LEAFY COTYLEDON1 (LEC1), WUSCHEL-related HOMEOBOX2 (WOX2) and SOMATIC EMBRYOGENESIS RECEPTOR-like KINASE (SERK) during somatic embryogenesis. Planta 243, 473-488.

Sangwan, R.S., Bourgeois, Y., Dubois, F., Sangwannorreel, B.S., 1992. INVITRO REGENERATION OF ARABIDOPSIS-THALIANA FROM CULTURED ZYGOTIC EMBRYOS AND ANALYSIS OF REGENERANTS. Journal of Plant Physiology 140, 588-595.

Sarkar, A.K., Luijten, M., Miyashima, S., Lenhard, M., Hashimoto, T., Nakajima, K., Scheres, B., Heidstra, R., Laux, T., 2007. Conserved factors regulate signalling in Arabidopsis thaliana shoot and root stem cell organizers. Nature 446, 811-814.

Song, Y.L., 2014. Insight into the mode of action of 2,4-dichlorophenoxyacetic acid (2,4-D) as an herbicide. Journal of Integrative Plant Biology 56, 106-113.

Steward, F.C., Mapes, M.O., Kent, A.E., Holsten, R.D., 1964. GROWTH + DEVELOPMENT OF CULTURED PLANT CELLS - BIOCHEMICAL + MORPHOGENETIC STUDIES WITH CELLS YIELD NEW EVIDENCE ON THEIR METABOLISM + TOTIPOTENCY. Science 143, 20-&.

Steward, F.C., Mapes, M.O., Smith, J., 1958. GROWTH AND ORGANIZED DEVELOPMENT OF CULTURED CELLS .1. GROWTH AND DIVISION OF FREELY SUSPENDED CELLS. American Journal of Botany 45, 693-703.

Stone, S.L., Kwong, L.W., Yee, K.M., Pelletier, J., Lepiniec, L., Fischer, R.L., Goldberg, R.B., Harada, J.J., 2001. LEAFY COTYLEDON2 encodes a B3 domain transcription factor that induces embryo development. Proceedings of the National Academy of Sciences of the United States of America 98, 11806-11811.

Su, Y.H., Liu, Y.B., Bai, B., Zhang, X.S., 2015. Establishment of embryonic shoot-root axis is involved in auxin and cytokinin response during Arabidopsis somatic embryogenesis. Frontiers in Plant Science 5, 9.

Su, Y.H., Su, Y.X., Liu, Y.G., Zhang, X.S., 2013. Abscisic acid is required for somatic embryo initiation through mediating spatial auxin response in Arabidopsis. Plant Growth Regulation 69, 167-176.

Su, Y.H., Zhao, X.Y., Liu, Y.B., Zhang, C.L., O'Neill, S.D., Zhang, X.S., 2009. Auxin-induced WUS expression is essential for embryonic stem cell renewal during somatic embryogenesis in Arabidopsis. Plant Journal 59, 448-460.

Szakonyi, D., Byrne, M.E., 2011. Ribosomal protein L27a is required for growth and patterning in Arabidopsis thaliana. Plant Journal 65, 269-281.

Tanaka, M., Kikuchi, A., Kamada, H., 2008. The Arabidopsis histone deacetylases

HDA6 and HDA19 contribute to the repression of embryonic properties after germination. Plant Physiology 146, 149-161.
Thibaud-Nissen, F.O., Shealy, R.T., Khanna, A., Vodkin, L.O., 2003. Clustering of microarray data reveals transcript patterns associated with somatic embryogenesis in soybean. Plant Physiology 132, 118-136.
Tsuwamoto, R., Yokoi, S., Takahata, Y., 2010. Arabidopsis EMBRYOMAKER encoding an AP2 domain transcription factor plays a key role in developmental change from vegetative to embryonic phase. Plant Molecular Biology 73, 481-492.
Ueda, M., Zhang, Z.J., Laux, T., 2011. Transcriptional Activation of Arabidopsis Axis Patterning Genes WOX8/9 Links Zygote Polarity to Embryo Development. Developmental Cell 20, 264-270.
Ulmasov, T., Murfett, J., Hagen, G., Guilfoyle, T.J., 1997. Aux/IAA proteins repress expression of reporter genes containing natural and highly active synthetic auxin response elements. Plant Cell 9, 1963-1971.
vandenBerg, C., Willemsen, V., Hendriks, G., Weisbeek, P., Scheres, B., 1997. Short-range control of cell differentiation in the Arabidopsis root meristem. Nature 390, 287-289.
Verdeil, J.L., Alemanno, L., Niemenak, N., Tranbarger, T.J., 2007. Pluripotent versus totipotent plant stem cells: dependence versus autonomy? Trends in Plant Science 12, 245-252.
Wang, G.D., Fiers, M., 2010. CLE peptide signaling during plant development. Protoplasma 240, 33-43.
Wickramasuriya, A.M., Dunwell, J.M., 2015. Global scale transcriptome analysis of Arabidopsis embryogenesis in vitro. Bmc Genomics 16, 23.
Wolters, H., Anders, N., Geldner, N., Gavidia, R., Jurgens, G., 2011. Coordination of apical and basal embryo development revealed by tissue-specific GNOM functions. Development 138, 117-126.
Wu, Y., Haberland, G., Zhou, C., Koop, H.U., 1992. SOMATIC EMBRYOGENESIS, FORMATION OF MORPHOGENETIC CALLUS AND NORMAL DEVELOPMENT IN ZYGOTIC EMBRYOS OF ARABIDOPSIS-THALIANA INVITRO. Protoplasma 169, 89-96.
Xiong, L.M., Lee, H.J., Ishitani, M., Zhu, J.K., 2002. Regulation of osmotic stress-responsive gene expression by the LOS6/ABA1 locus in Arabidopsis. Journal of Biological Chemistry 277, 8588-8596.
Zhang, Z.J., Tucker, E., Hermann, M., Laux, T., 2017. A Molecular Framework for the Embryonic Initiation of Shoot Meristem Stem Cells. Developmental Cell 40, 264-277.

Zimmerman, J.L., 1993. SOMATIC EMBRYOGENESIS - A MODEL FOR EARLY DEVELOPMENT IN HIGHER-PLANTS. Plant Cell 5, 1411-1423.
Zuo, J.R., Niu, Q.W., Frugis, G., Chua, N.H., 2002. The WUSCHEL gene promotes vegetative-to-embryonic transition in Arabidopsis. Plant Journal 30, 349-359.
Zurcher, E., Tavor-Deslex, D., Lituiev, D., Enkerli, K., Tarr, P.T., Muller, B., 2013. A Robust and Sensitive Synthetic Sensor to Monitor the Transcriptional Output of the Cytokinin Signaling Network in Planta. Plant Physiology 161, 1066-1075.

Figure legends

Figure 1. Characteristics of callus tissue and embryonic structures formed in shoot apex explants and the SE formation rate. *(A) Schematic diagram of SE induction from the shoot apex. For standard induction, two cotyledonary petioles were cut off from the shoot apex explant (approximately 1 mm in length). For microscopic observation, one cotyledon was removed from the shoot apex explant to expose the SAM. The explants were cultured on stress medium containing 0.7 M mannitol for 6 h and then incubated on E4.5 medium containing 4.5 M 2,4-D. Time-lapse microscopic observation was carried out at days 1–5 on E4.5 medium (SE induction). (B–E) After 12 days of incubation on E4.5 medium, the explants*

were categorized into four groups based on their morphology and the presence/absence of a SE: smooth surface callus (SSC) with SE (B), SSC without SE (C), rough surface callus (RSC) (D), and dead tissues (E). Two representative samples of each group are shown. (F) The rate for each category of explants derived from 4DAS-stage seedlings. The SE-formation ratio was 20% (± 3.33% s.d., n = 90 explants). (G) Time-lapse images of an SE-forming explant. The images were taken at days 1, 3, 5, 7 and 9 of SE induction in the same explant. Black arrowheads and white arrows indicate embryonic structures and the first and second true leaves, respectively. (H) Staining of seeds, explants with SEs and RSC, and untreated seedling (6DAS) with Sudan Red 7B. Scale bars: 1 mm (B–E, H; SE, RSC, and Seedling) and 500 μm (G and H; Seed).

Figure 2. Expression of phytohormone-related reporters in explants with or without SE formation. *Expression patterns of the reporters pPIN1::PIN1-GFP (A), pDR5rev::3XVENUS-N7 (B) and pTCSn::tdTomato-N7 (C) at days 1–5 of SE induction. Upper panels are SE-forming explants and lower panels are non-forming explants. Yellow and red arrows indicate SE-forming regions and SAMs, respectively. For pPIN1::PIN1-GFP and pDR5rev::3XVENUS-N7 detection (A and B), the reporter signals are in green and chlorophyll autofluorescence is in magenta.*

After osmotic stress application, the damaged cells exhibited autofluorescence, which was detected in both the magenta and green channels and is colored white in the merged figures. For pTCSn::tdTomato-N7 (C), the reporter signal is in magenta and chlorophyll autofluorescence is in green. All images are projection views of Z-stack sections. Scale bars: 200 μm (A–C).

Figure 3. Expression of apical meristem markers in SE-forming explants. *(A, B) Expression patterns of pWUS::dsRed-N7, pCLV3::dsRed-N7, pWOX5::GFP-er (A) and pDRN::erGFP (B) at days 1–5 of SE induction. (A) pWUS::dsRed-N7 and pCLV3::dsRed-N7 signals are in magenta and pWOX5::GFP-er signals are in green. After osmotic stress application, the damaged cells exhibited autofluorescence, which was also detected in the green channel, but the reporter signal was distinguished from the autofluorescence by its ER-localization pattern. (B) The pDRN::erGFP signal and chlorophyll autofluorescence are in green and magenta, respectively. All images show the projection of Z-stack sections. The (a), (b), and (d) panels show enlarged images of part of the day 2, day 3 and day 5 images of pWUS::dsRed-N7/pWOX5::GFP-er explant. The (c) panel shows an enlarged image of part of the day 4 image of a pCLV3::dsRed-N7 explant. The (e to h) panels show enlarged images of part of the day 2–5 images of pDRN::erGFP explant. Scale*

bars: 200 μm (A and B) and 100 μm (a–h).

Figure 4. Expression of embryonic markers in SE-forming explants and selection of SE-forming and non-SE-forming explants. *(A) The expression patterns of pLEC1::LEC1-GFP and pWOX2::NLS-YFP at days 1–5 of SE induction. pLEC1::LEC1-GFP and pWOX2::NLS-YFP signals are in green and the autofluorescence signal is in magenta. After osmotic stress application, the damaged cells exhibited an autofluorescence signal, which was detected in both the magenta and green channels and is colored white in the merged figure. Yellow arrows indicate the reporter signals. (B) Expression pattern of pWOX2::NLS-YFP in SE-forming and non-forming explants at day 3. (C) Rates of SE formation in explants sorted by pWOX2::NLS-YFP expression at day 3 of SE induction. Explants showing a clear signal with nuclear localization at day 3 were sorted as "day3 positive", while the explants showing no signal or a very weak signal without nuclear localization were sorted as "day3 negative". All explants were assessed for SE formation by Sudan Red staining at day 8. Six batches of experiments (n ≥ 25 for each batch) were performed and the results of the middle-ranked four batches were used to create the bar graph. Scale bars: 200 um (A and upper panels in B) and 50 um (lower panels in B).*

Figure 5. Expression of various markers in SE-forming explants at day 3. *(A–C) Expression patterns of pWOX2::NLS-YFP (A), pPIN1::PIN1-GFP (B), and pWUS::dsRed-N7/pWOX5::GFP-er (C) at day 3 of SE induction. (C') Enlarged image of part of (C). The (A–C) panels show a projection of Z-stack sections. The (C') panel is a single optical section. Cellular outlines were visualized with PI staining. The letter p indicates the third and fourth true leaf primordia. Scale bars: 100 µm (A–C) and 50 µm (C').*

Figure 6. Expression changes of key developmental genes for embryos and shoot and root meristems during SE induction. *(A) Scheme of sample collection for transcriptome analysis. (B) Clustering display of expression intensities of key genes for embryonic development. (C) Clustering display of expression intensities of key developmental genes for the shoot apical meristem. (D) Clustering display of expression intensities of key developmental genes for the root meristem.*

Figure 7. Gene expression patterns of SE-enriched genes in plant development. *(A) Venn diagram of the genes enriched in SE-forming explants at day 3 and day 5. By comparing SE-forming explants and non-SE-forming explants at each stage (day 3 and day 5), 73 genes were identified as enriched in day 3 SE-forming explants (FC > 1.5, $p < 0.05$) and 159 genes as enriched in day 5 SE-forming explants (FC > 1.5,*

p < 0.05). (B) Heat map showing the clustering results for the 73 genes enriched in day 3 SE-forming explants, using previously reported expression data sets in wild-type seed tissues (Belmonte et al., 2013), root tissues (Birnbaum et al., 2003) and a microarray data set from AtGenExpress (TAIR Accession: ExpressionSet:1006710873; https://www.arabidopsis.org/servlets/TairObject?type=expression_set&id=1006710873). All gene data sets were normalized to the expression intensity of PP2A (AT1G69960). LRC, lateral root cap in the root tip region. The arrowhead indicates the data set from young lateral root cap cells in the root tip (referred to as lateral root cap stage1 in (Birnbaum et al., 2003) (C) Heat map showing the clustering result for the 159 genes enriched in day 5 SE-forming explants, using the same data sets as above. Arrowheads indicate data sets from seed compartments (embryo proper, micropylar endosperm, peripheral endosperm, chalazal endosperm, seed coat) at the mature green stage (Belmonte et al., 2013). (D) Clustering display of expression intensities of SE-enriched genes (day 3) highly expressed in the root tip LRC in (B).

Figure 8. Overview of the shoot apex-derived SE induction system *(A) Schematic diagrams of shoot apex explants and expression changes of shoot meristem genes,*

key embryonic genes, and root genes during SE induction. In SE-forming explants, SE specification takes place during the period around day 3 (green dotted line), where the explants possessed a mixed identity (shoot, root and embryo). In non-forming explants, embryonic genes are not expressed and the root genes are not yet highly expressed in this period (blue dotted line). (B) Schematic diagram of reporter expression at day 3 (auxin, apical meristem and embryonic markers) and day 5 (cytokinin).

Supplemental Figures

Figure S1. Expression of apical meristem markers in non-SE explants. *(A, B) Expression patterns of pWUS::dsRed-N7/pWOX5::GFP-er (A) and pDRN::erGFP (B) in non-SE-forming explants at days 1–5 of SE induction. (A) The pWUS::dsRed-N7 signal is in magenta. The pWOX5::GFP-er signal is in green. After osmotic stress application, the damaged cells exhibited an autofluorescence signal, which was also detected in the green channel, but the reporter signal was distinguished from the autofluorescence signal by its ER-localization pattern. (B) The pDRN::erGFP signal is in green and chlorophyll autofluorescence is in magenta. All the images are projection views of Z-stack sections.*

Figure S2. Expression of embryonic markers in non-SE-forming explants

Expression patterns of pLEC1::LEC1-GFP and pWOX2::NLS-YFP in non-SE-forming explants at days 1–5 of SE induction. pLEC1::LEC1-GFP and pWOX2::NLS-YFP signals are in green and autofluorescence is in magenta. After osmotic stress application, the damaged cells exhibited autofluorescence, which was detected in both the magenta and green channels and is colored white in the merged figure.

Figure S3. Gene expression level of WOX2 in SE-forming and non-SE-forming explants *The expression level of WOX2 in SE-forming and non-SE-forming explants at day 3 and day 5 (day3_positive, day3_negative, day5_positive and day5_negative) was detected by RNA-seq.*

Figure S4. Heat maps for SE-enriched genes with the data sets normalized to ACT7 *(A) Heat map showing the clustering results for 73 genes enriched in day 3 SE-forming explants compared with non-SE-forming explants (FC > 1.5, p < 0.05), using previously reported expression data sets in wild-type seed tissues (Belmonte et al., 2013), root tissues (Birnbaum et al., 2003) and a microarray data set from AtGenExpress (TAIR Accession:ExpressionSet:1006710873;https://www.arabidopsis.org/servlets/TairObject?type=expression_set&id=1006710873). All gene data sets were normalized to*

the expression intensity of ACT7 (AT5G09810). The arrowhead indicates the data set from young lateral root cap cells in the root tip (referred to as lateral root cap at stage1 in (Birnbaum et al., 2003). (B) Heat map showing the clustering results for 159 genes enriched in day 5 SE-induced explants compared with non-SE-forming explants (FC > 1.5, p < 0.05). Arrowheads indicate data sets from seed compartments (embryo proper, micropylar endosperm, peripheral endosperm, chalazal endosperm and seed coat) at the mature green stage (Belmonte et al., 2013).

Figure S5. Heat maps for SE-enriched genes with the data sets normalized to UBI10 *(A) Heat map showing the clustering results for 73 genes enriched in day 3 SE-forming explants compared with non-SE-forming explants (FC > 1.5, p < 0.05), using previously reported expression data sets in wild-type seed tissues (Belmonte et al., 2013), root tissues (Birnbaum et al., 2003) and a microarray data set from AtGenExpress (TAIR Accession:ExpressionSet:1006710873;https://www.arabidopsis.org/servlets/TairObject?type=expression_set&id=1006710873). All gene data sets were normalized to the expression intensity of UBI10 (AT4G05320). The arrowhead indicates the data set from young lateral root cap cells in the root tip (referred to as lateral root cap at*

stage1 in (Birnbaum et al., 2003) (B) Heat map showing the clustering results for 159 genes enriched in day 5 SE-induced explants compared with non-SE-forming explants (FC > 1.5, p < 0.05). Arrowheads indicate data sets from seed compartments (embryo proper, micropylar endosperm, peripheral endosperm, chalazal endosperm and seed coat) at the mature green stage (Belmonte et al., 2013)

Figure S6. Expression changes of LRC genes during SE induction. *Clustering display of the expression intensities of LRC-enriched genes reported in (Brady et al., 2007).*

Figure S7. Real time qRT-PCR for validation of RNA-seq. *(A–C) Relative gene expression levels of LEC1, SMB and WOX2 in the explants (shoot apex, stress, day 3 positive, day 3 negative, day 5 positive and day 5 negative) quantified by qRT-PCR. (C') The expression levels of WOX2 at day 3 and day 5 in (C) are shown in (C') with different scale intervals on the y-axis.*

Figure 1

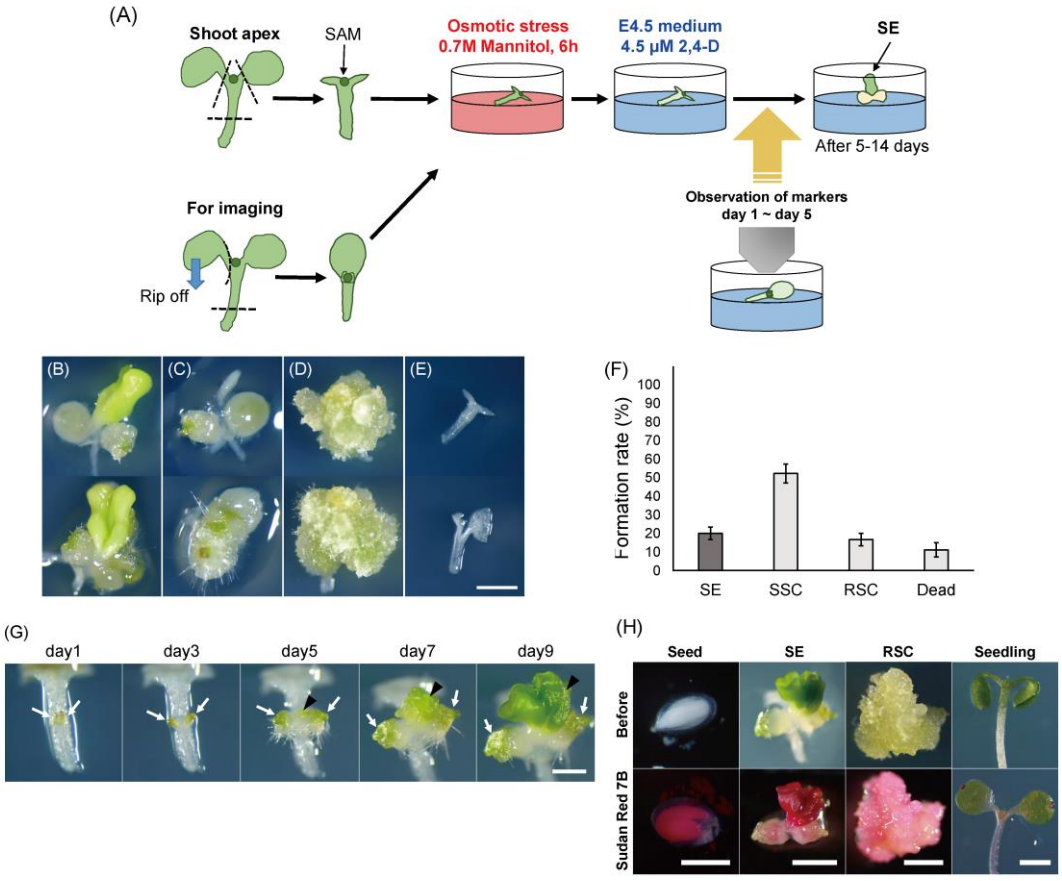
(A)
Shoot apex
SAM
Osmotic stress
0.7M Mannitol, 6h
E4.5 medium
4.5 μM 2,4-D
SE
After 5-14 days
Observation of markers
day 1 ~ day 5
For imaging
Rip off
(B)
(C)
(D)
(E)
(F)
Formation rate (%)
100
90
80
70
60
50
40
30
20
10
0
SE
SSC
RSC
Dead
(G)
day1
day3
day5
day7
day9
(H)
Seed
SE
RSC
Seedling
Before
Sudan Red 7B

Figure 2

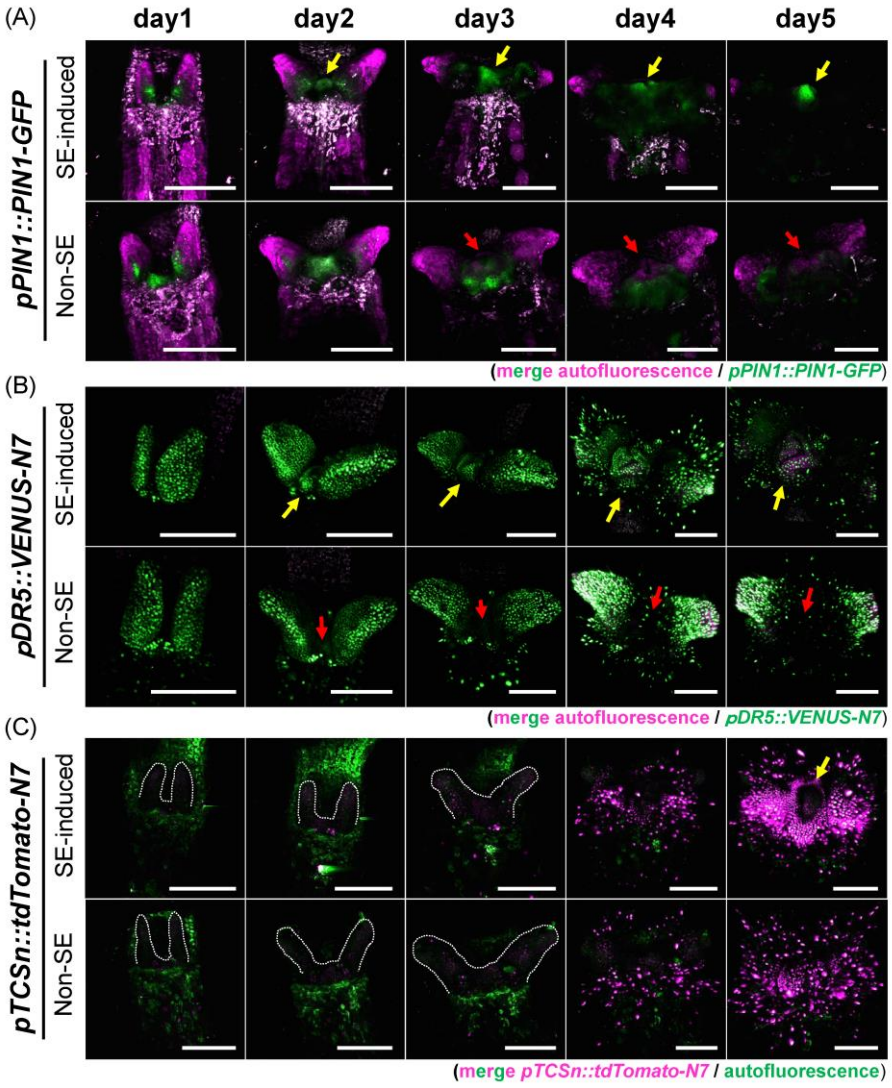
(A)
day1
day2
day3
day4
day5
pPIN1::PIN1-GFP
SE-induced
Non-SE
(merge autofluorescence / pPIN1::PIN1-GFP)
(B)
pDR5::VENUS-N7
SE-induced
Non-SE
(merge autofluorescence / pDR5::VENUS-N7)
(C)
pTCSn::tdTomato-N7
SE-induced
Non-SE
(merge pTCSn::tdTomato-N7 / autofluorescence)

Figure 3

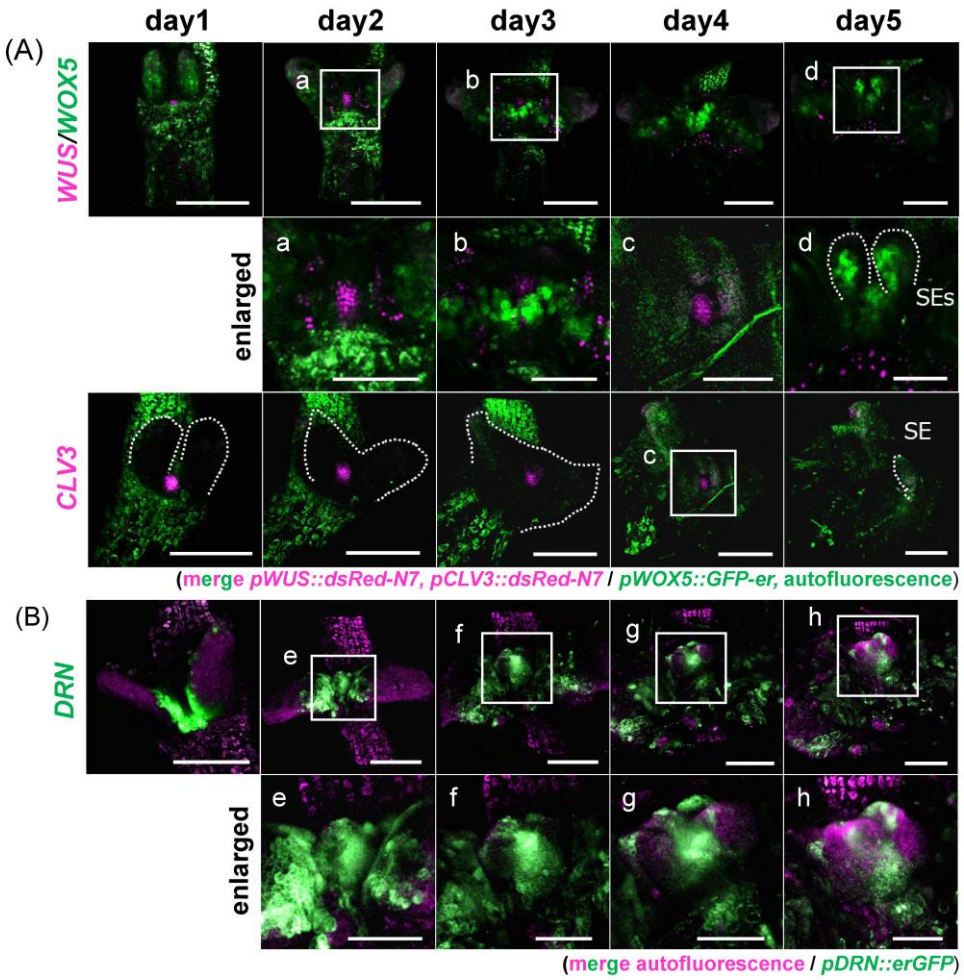
day1
day2
day3
day4
day5
(A)
WUS/WOX5
a
b
d
enlarged
a
b
c
d
SEs
CLV3
c
SE
(merge pWUS::dsRed-N7, pCLV3::dsRed-N7 / pWOX5::GFP-er, autofluorescence)
(B)
DRN
e
f
g
h
enlarged
e
f
g
h
(merge autofluorescence / pDRN::erGFP)

Figure 4

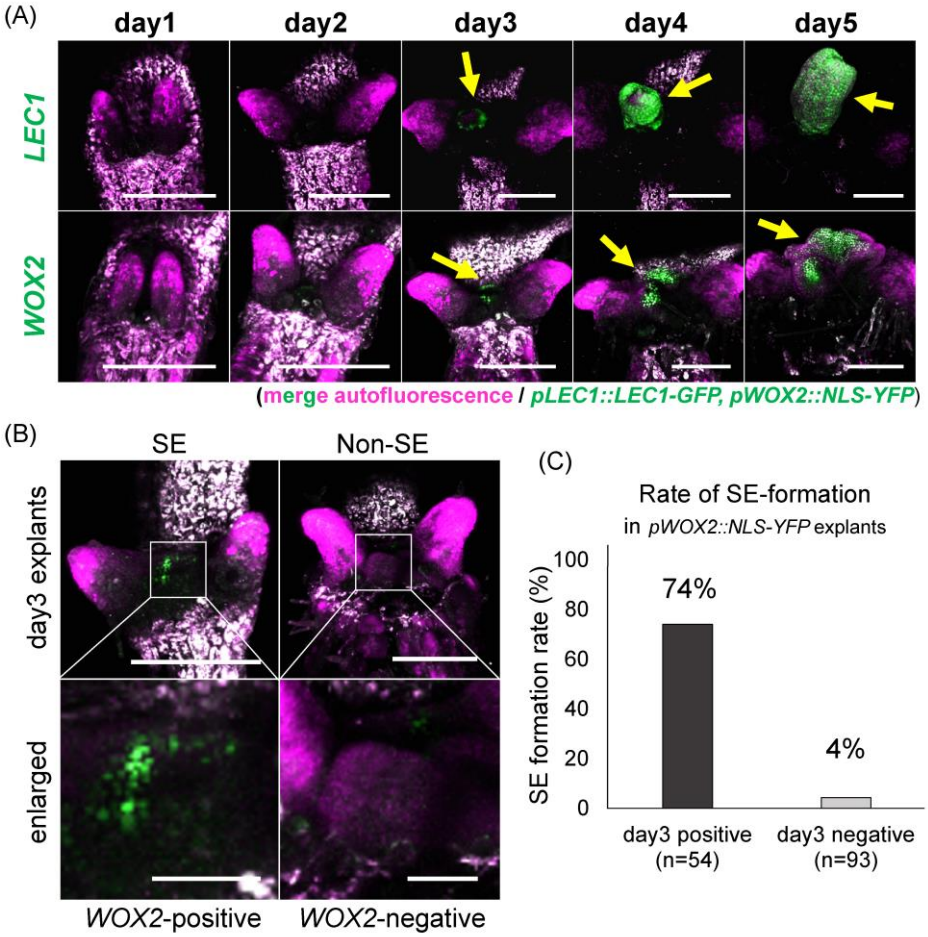
(A)
day1
day2
day3
day4
day5
LEC1
WOX2
(merge autofluorescence / pLEC1::LEC1-GFP, pWOX2::NLS-YFP)
(B)
SE
Non-SE
day3 explants
enlarged
WOX2-positive
WOX2-negative
(C)
Rate of SE-formation
in pWOX2::NLS-YFP explants
SE formation rate (%)
100
80
60
40
20
0
74%
4%
day3 positive
(n=54)
day3 negative
(n=93)

Figure 5

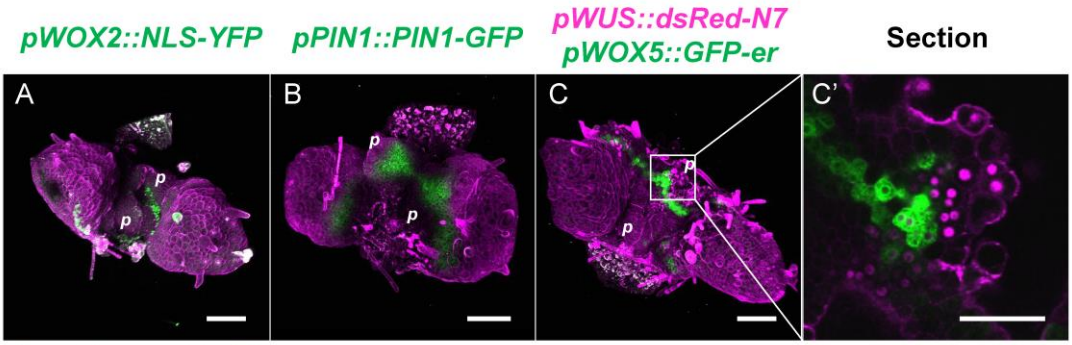

Figure 6

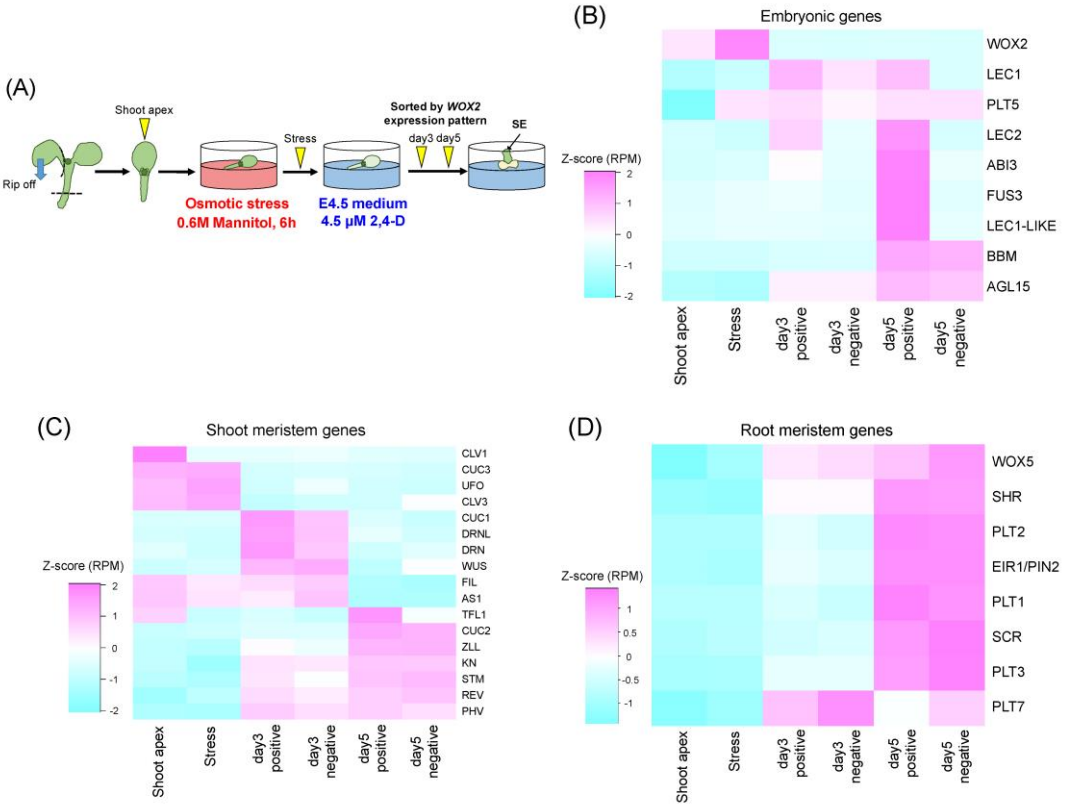
(A)
Shoot apex
Rip off
Stress
Sorted by WOX2 expression pattern
day3 day5
SE
Osmotic stress
0.6M Mannitol, 6h
E4.5 medium
4.5 µM 2,4-D
(B)
Embryonic genes
Z-score (RPM)
WOX2
LEC1
PLT5
LEC2
ABI3
FUS3
LEC1-LIKE
BBM
AGL15
Shoot apex
Stress
day3 positive
day3 negative
day5 positive
day5 negative
(C)
Shoot meristem genes
Z-score (RPM)
CLV1
CUC3
UFO
CLV3
CUC1
DRNL
DRN
WUS
FIL
AS1
TFL1
CUC2
ZLL
KN
STM
REV
PHV
(D)
Root meristem genes
Z-score (RPM)
WOX5
SHR
PLT2
EIR1/PIN2
PLT1
SCR
PLT3
PLT7

Figure 7

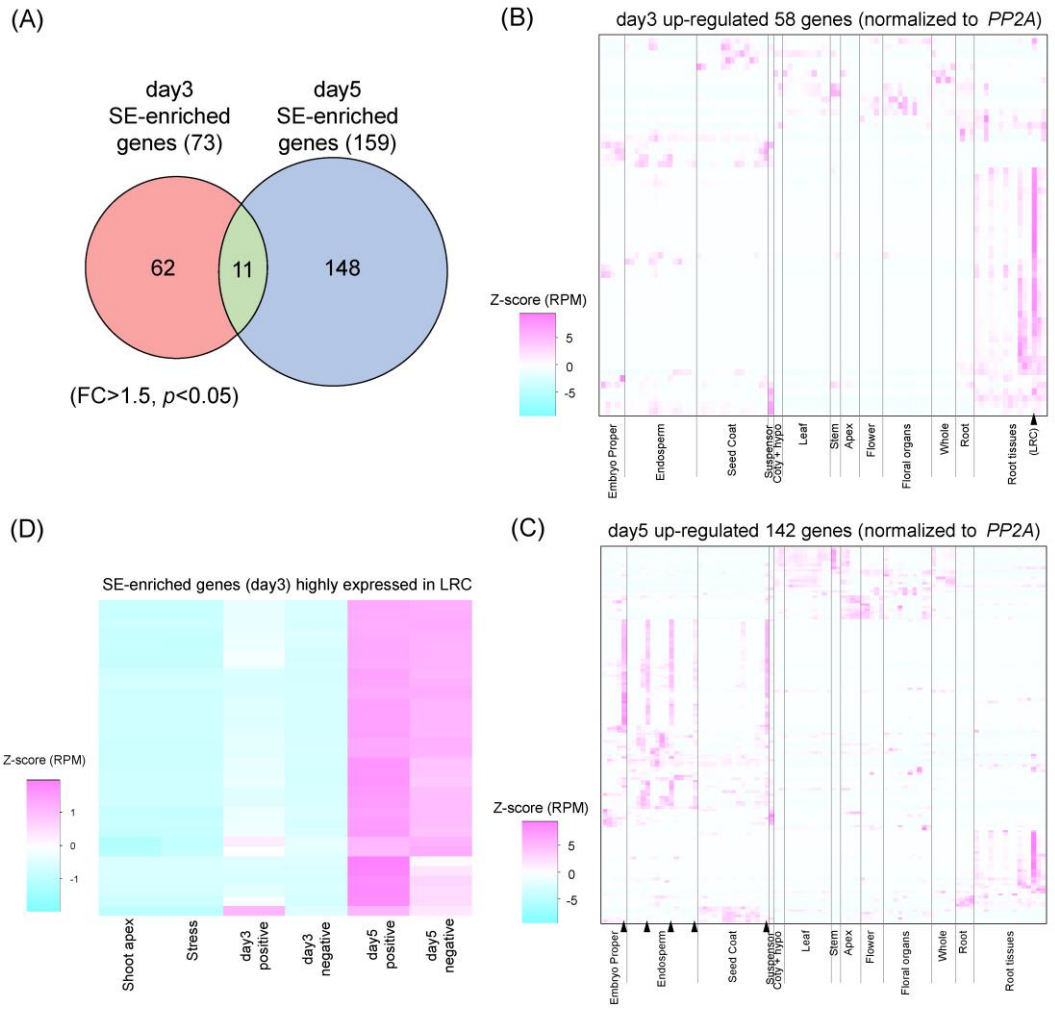
(A)
day3 SE-enriched genes (73)
day5 SE-enriched genes (159)
62
11
148
(FC>1.5, p<0.05)
(B)
day3 up-regulated 58 genes (normalized to PP2A)
Z-score (RPM)
5
0
-5
Embryo Proper
Endosperm
Seed Coat
Suspensor
Cotyl + hypo
Leaf
Stem
Apex
Flower
Floral organs
Whole
Root
Root tissues
(LRC)
(D)
SE-enriched genes (day3) highly expressed in LRC
Z-score (RPM)
1
0
-1
Shoot apex
Stress
day3 positive
day3 negative
day5 positive
day5 negative
(C)
day5 up-regulated 142 genes (normalized to PP2A)
Z-score (RPM)
5
0
-5
Embryo Proper
Endosperm
Seed Coat
Suspensor
Cotyl + hypo
Leaf
Stem
Apex
Flower
Floral organs
Whole
Root
Root tissues

Figure 8

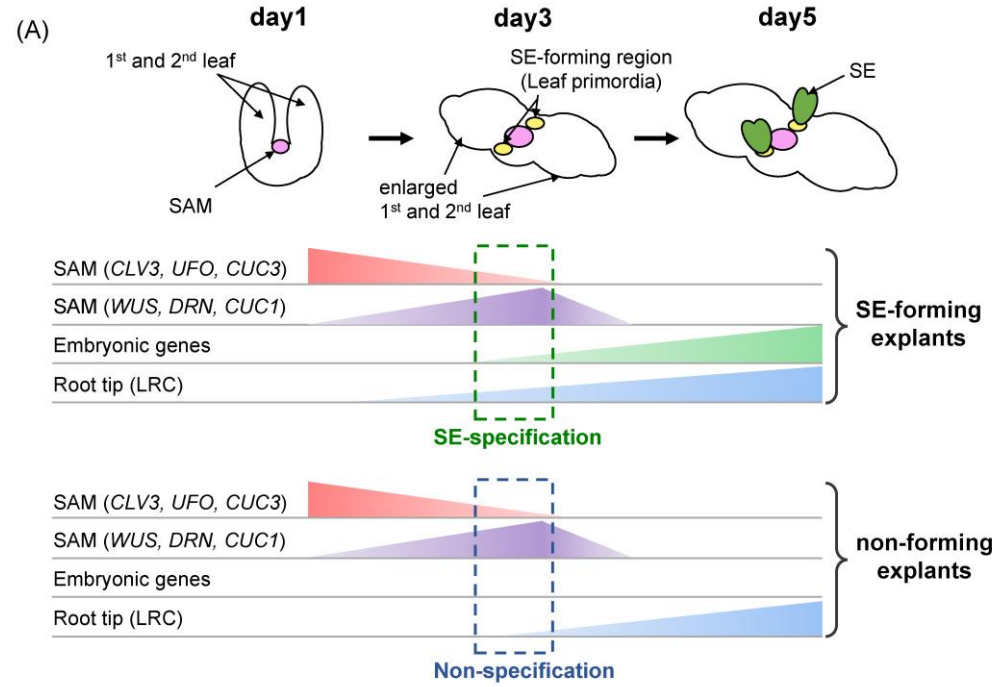
(A)
day1
day3
day5
1st and 2nd leaf
SAM
SE-forming region
(Leaf primordia)
enlarged
1st and 2nd leaf
SE
SAM (CLV3, UFO, CUC3)
SAM (WUS, DRN, CUC1)
Embryonic genes
Root tip (LRC)
SE-forming explants
SE-specification
SAM (CLV3, UFO, CUC3)
SAM (WUS, DRN, CUC1)
Embryonic genes
Root tip (LRC)
non-forming explants
Non-specification

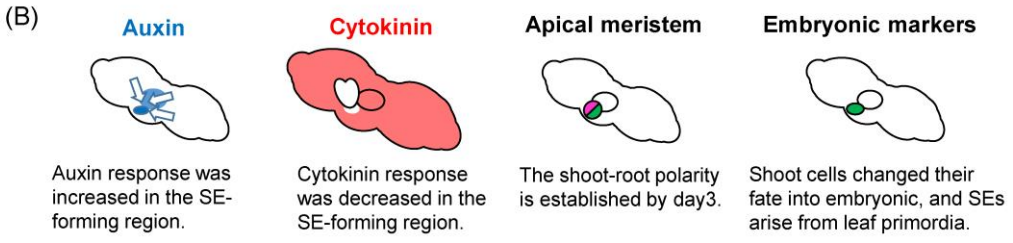
(B)
Auxin
Cytokinin
Apical meristem
Embryonic markers
Auxin response was increased in the SE-forming region.
Cytokinin response was decreased in the SE-forming region.
The shoot-root polarity is established by day3.
Shoot cells changed their fate into embryonic, and SEs arise from leaf primordia.

Highlights:

- Somatic embryogenesis derived from shoots includes drastic fate conversion process
- Somatic embryo arises from the leaf primordia beside the shoot apical meristem
- Somatic embryo initiates without the intermediate process of callus formation
- Only a limited number of transcripts are specific to embryo-forming explants
- The explants possess a mixed identity at the time of embryonic fate specification